Evolution, 2023, **77(3)**, 852–869
https://doi.org/10.1093/evolut/qpac068
Advance access publication 28 December 2022
Original Article

Hybrid zone or hybrid lineage: a genomic reevaluation of Sibley's classic species conundrum in *Pipilo* towhees

Devon A. DeRaad[1], Emily E. Applewhite[2], Whitney L.E. Tsai[2], Ryan S. Terrill[2], Sarah E. Kingston[3,4,5], Michael J. Braun[3,4], John E. McCormack[2]

[1]Biodiversity Institute and Department of Ecology and Evolutionary Biology, University of Kansas, Lawrence, KS, United States
[2]Moore Laboratory of Zoology, Occidental College, Los Angeles, CA, United States
[3]Department of Vertebrate Zoology, National Museum of Natural History, Smithsonian Institution, Washington, DC, United States
[4]Behavior, Ecology, Evolution and Systematics Program, University of Maryland, College Park, MD, United States
[5]Sea Education Association, Woods Hole, MA, United States

Corresponding author: Moore Laboratory of Zoology, Occidental College, Los Angeles, CA 90041, United States. Email: mccormack@oxy.edu

Abstract

Hybrid zones can be studied by modeling clines of trait variation (e.g., morphology, genetics) over a linear transect. Yet, hybrid zones can also be spatially complex, can shift over time, and can even lead to the formation of hybrid lineages with the right combination of dispersal and vicariance. We reassessed Sibley's (1950) gradient between Collared Towhee (*Pipilo ocai*) and Spotted Towhee (*Pipilo maculatus*) in Central Mexico to test whether it conformed to a typical tension-zone cline model. By comparing historical and modern data, we found that cline centers for genetic and phenotypic traits have not shifted over the course of 70 years. This equilibrium suggests that secondary contact between these species, which originally diverged over 2 million years ago, likely dates to the Pleistocene. Given the amount of mtDNA divergence, parental ends of the cline have very low autosomal nuclear differentiation (F_{ST} = 0.12). Dramatic and coincident cline shifts in mtDNA and throat color suggest the possibility of sexual selection as a factor in differential introgression, while a contrasting cline shift in green back color hints at a role for natural selection. Supporting the idea of a continuum between clinal variation and hybrid lineage formation, the towhee gradient can be analyzed as one population under isolation-by-distance, as a two-population cline, and as three lineages experiencing divergence with gene flow. In the middle of the gradient, a hybrid lineage has become partly isolated, likely due to forested habitat shrinking and fragmenting as it moved upslope after the last glacial maximum and a stark environmental transition. This towhee system offers a window into the potential outcomes of hybridization across a dynamic landscape including the creation of novel genomic and phenotypic combinations and incipient hybrid lineages.

Keywords: secondary contact, incipient speciation, divergence with gene flow, hybrid speciation, differential introgression, speciation

Introduction

> "If all animals currently displayed the patterns of variation that have been described in the Mexican red-eyed towhees, it would be impossible ever to arrive at a species concept. It is fortunate, however, that a few examples of this type are available for study, for they present the natural proving grounds for the Neo-Darwinian theory of species formation."
>
> Charles G. Sibley (1950)

Hybrid zones have long been proving grounds for evolutionary theory (Barton & Hewitt, 1985; Harrison & Harrison, 1993; Hewitt, 1988; Mallet & Barton, 1989). Advances in cline theory provided a mathematical framework for the study of hybrid zones (Barton, 1979; Endler, 1977). But clinal variation across hybrid zones—the changes in traits across a linear transect—is also a simplification of complex phenomena that vary in both space and time. Recently, genomic data have exposed the vast array of potential outcomes when hybridization occurs in nature (Taylor & Larson, 2019), including dynamic shifts across time periods (Wielstra, 2019), asymmetric introgression of advantageous traits (Bennett et al., 2021), and gene flow on a complex landscape involving more than two species (Pardo-Diaz et al., 2012). Phylogenomic data are also revealing that many organismal radiations bear the hallmark of ancient hybridization (Barley et al., 2022; DeRaad et al., 2022; Ferreira et al., 2021; Meier et al., 2017) and many modern species are products of significant genetic introgression (Racimo et al., 2015; Schumer et al., 2018) or even hybrid speciation (Mallet, 2007).

Despite advances in our understanding of hybridization, the connection between long-studied hybrid zones and evolutionary radiations comprised of species showing evidence for introgression remains murky. Given the dynamic climate history of the Quaternary, several scenarios are imaginable where hybrid zones could contribute to hybrid lineage formation. In one scenario, lineages in the process of speciation might come back into contact, exchanging genes for a while, before diverging again through vicariance, producing reticulate evolution in gene trees and discordance with the species phylogeny (Cui et al., 2013; Good et al., 2003). Another possibility is that portions of a hybrid zone might become isolated through vicariance, leaving behind hybrid lineages on

Received November 3, 2022; revisions received December 16, 2022; accepted December 24, 2022

their own evolutionary trajectory (Dowling & Secor, 1997; Hermansen et al., 2011; Ottenburghs, 2018).

Some recent empirical studies suggest that when hybrid zones shift or break apart, they can leave behind isolated lineages of hybrid origin. In western North America, Common Ravens (*Corvus corax*) are a mosaic lineage formed from ancient hybridization between non-sister species (Kearns et al., 2018). Likewise, the Italian Sparrow (*Passer italiae*) likely formed as a hybrid species when House Sparrows (*P. domesticus*) and Spanish Sparrows (*P. hispaniolensis*) came into contact (Hermansen et al., 2011), although the species is now largely isolated reproductively and geographically. So far, examples of hybrid zones spawning isolated hybrid lineages are few and often controversial because they involve assumptions about the prior geographic ranges of modern species. To better understand the link between hybrid zones and hybrid lineage formation, we need more examples of hybrid zones experiencing vicariance.

In the 1940s, Charles Sibley embarked on one of the first and still most classic studies of avian hybridization between what are now called the Collared Towhee (*Pipilo ocai*) and Spotted Towhee (*Pipilo maculatus*) in Mexico. The system had many compelling features to suit Sibley's goal of studying "the species problem." Both species are distributed in montane forests, with varying degrees of hybridization where they come into contact. The most well-studied of these contact areas stretches across the Trans-Mexican Volcanic Belt (TMVB) from Collared Towhee populations in the west to Spotted Towhee populations in the east (Figure 1A). Sibley's plots of trait change along this hybrid gradient (Sibley, 1950, 1954) were striking, influencing both the modern synthesis (Dobzhansky, 1955; Mayr, 1963) and the development of cline theory (Endler, 1977).

Since Sibley's pioneering work, genetic studies have validated and extended many of his conclusions, especially the clinal nature of variation in both phenotypic traits and genetic loci in the towhees (Kingston et al., 2012; Kingston et al., 2014). Yet, both Sibley's data and modern work contain hints that the situation might be more complex than a simple cline and could involve both vicariance and incipient lineage formation. Sibley (1950) recognized subspecies breaks in the phenotypic clines, and genetic ancestry based on amplified fragment length polymorphisms suggested population substructure across the TMVB (Kingston et al., 2014). A phenotypically stable form in the eastern part of the TMVB is recognized by some ornithologists as a distinct taxon, called the Olive-backed Towhee (Howell & Webb, 1995), which might overlap geographically with a subspecies of the Spotted Towhee (*P. maculatus macronyx*). A more complete understanding of this gradient, integrating phenotypic, genomic, and environmental data, would help distinguish whether this case of secondary contact is best described by a model of continuous divergence, a sigmoidal cline model, or a multispecies model corresponding to geographic substructuring. Beyond helping resolve taxonomy, testing these competing models would reveal the evolutionary outcomes of secondary contact across a complex biogeographic landscape shedding light on the roles of specific isolating barriers and the ability of hybridization to generate a novel and lasting variation.

Our goal was to assess the spatial and temporal context of hybridization between the Collared Towhee and Spotted Towhee using modern and historical specimens spanning the TMVB (Figure 1A). We start by using cline models to analyze phenotype and genotype, both linked to a set of historical specimens spanning the gradient. While genetics and phenotype have been studied independently, they have never been analyzed together from the same specimens to understand genotype-phenotype associations and differential introgression patterns. Second, we test whether cline centers have shifted over 70 years by comparing our historical results to modern data (Kingston et al., 2014; Kingston et al., 2017), allowing us to determine whether introgression is operating on ecological timescales, perhaps the result of modern habitat alterations, as Sibley (1950) speculated, or evolutionary timescales more likely influenced by habitat shifts during glacial cycling. Next, we expand from cline models to assess evidence of lineage formation using phylogenetics, population genetics, and demographic modeling. Finally, we address the association between niche variation and genetic breaks using landscape-level environmental data associated with photo-vouchered observations.

Methods

Genetic and phenotypic data collection

For DNA analysis, we sampled 32 historical museum specimens, 4 individuals (or 8 alleles) from each of 8 populations across the TMVB (Table 1; Figure 1A) from Jalisco in the west to Puebla in the east (average distance between sites = 82 km; range = 40–116 km). Specimens from 7 of 8 sites were collected from 1939 to 1954 by Chester C. Lamb for the Moore Laboratory of Zoology at Occidental College. Specimens from one site derive from Sibley's original collections, which were made during a similar time period (1946–1950), and which Lamb's transect closely parallels. The sampling design also mirrors a modern transect collected from 2008 to 2009 (Kingston et al., 2014; Kingston et al., 2017).

We scored plumage traits of vouchered specimens for the 32 genotyped individuals and a broader sample of 74 individuals at the transect sites following the key published in Sibley (1950). Each trait received a value from 0 to 4, where 0 represents pure Collared Towhee phenotype, and 4 represents pure Spotted Towhee phenotype: pileum (0 = rufous cap; 4 = all-black head), back color (0 = green; 1 = black), throat color (0 = white; 4 = black), back spotting (0 = none; 4 = fully spotted), tail spotting (0 = none; 4 = fully spotted), and flanks (0 = gray; 4 = rufous).

DNA sequencing and SNP calling

We extracted DNA from a small fragment of the toepad of each specimen. We digested the samples and extracted DNA using phenol-chloroform (Tsai et al., 2020), with negative controls and strict protocols for preventing cross-contamination, including carrying out the extraction in a clean room using dedicated equipment and consumables. We performed library preparation using a Kapa kit (Kapa Biosystems, Inc.) with custom index tags (Glenn et al., 2019). We pooled eight samples for target enrichment using the tetrapod 5K ultraconserved element (UCE) probe set (Faircloth et al., 2012). We combined the enriched pools at equimolar ratios and sequenced on a partial lane of an Illumina HiSeq 2500 using 125 base pair, paired-end (PE125) sequencing. We obtained a total of 94 million read pairs with an average of 2.9 million read pairs per sample.

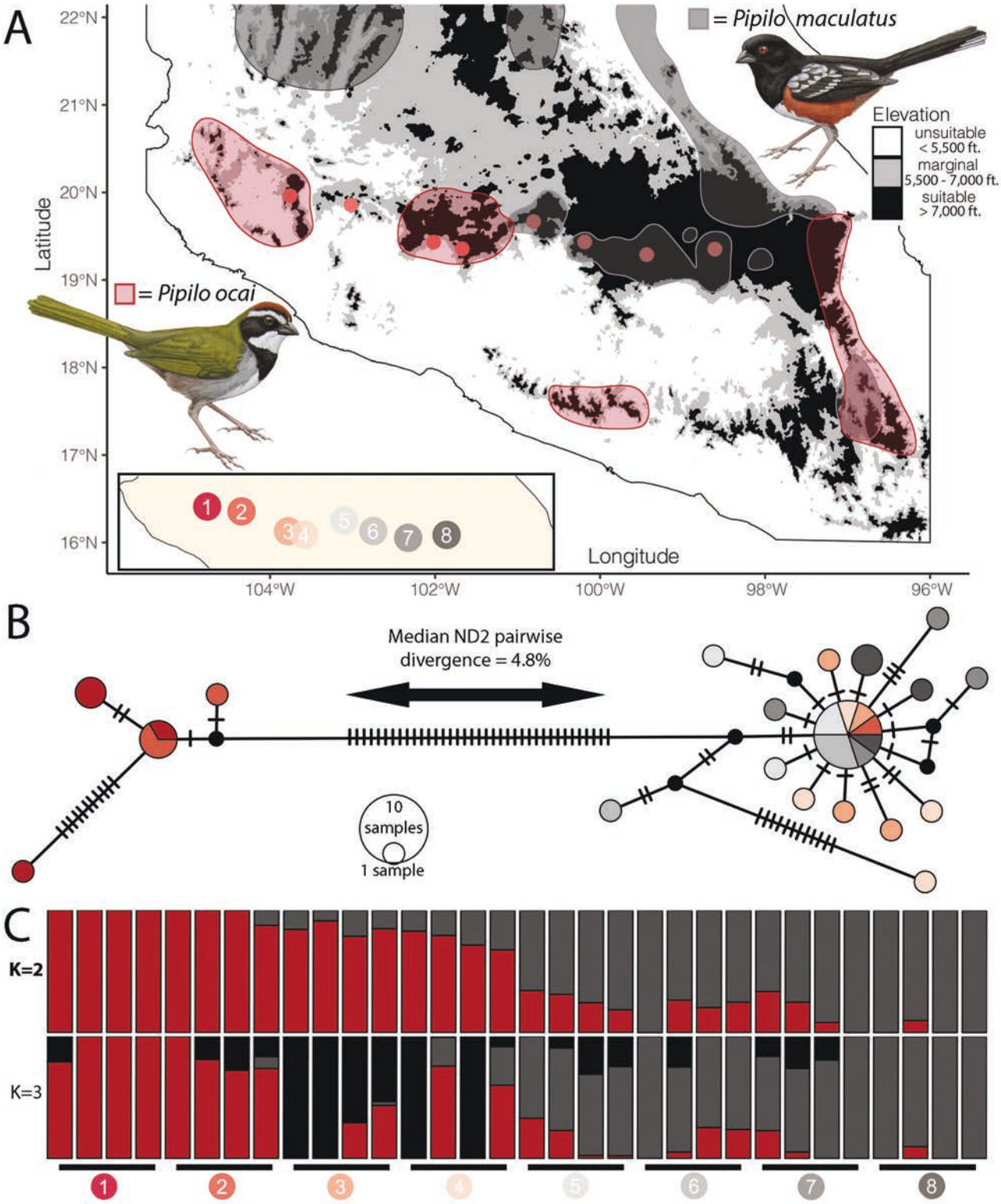

Figure 1. (A) Distribution map adapted from Sibley (1950), with the distribution of Spotted Towhee (*P. maculatus*) shown in gray and the distribution of Collared Towhee (*P. ocai*) shown in light red. The inset plot shows the eight genetic sampling localities. Towhee illustrations by Alex Warnick. (B) Haplotype network of the ND2 gene with hash marks indicating mutation steps. Pie colors represent the proportion of that haplotype represented in the eight populations. (C) ADMIXTURE plot showing the genetic assignment of each individual with two ($K = 2$) and three ($K = 3$) genetic clusters.

To assemble UCEs from raw reads, we used *illumiprocessor* (Faircloth, 2014), a wrapper around the program *trimmomatic* v.0.39.1 (Bolger et al., 2014), to clean and trim raw reads. We then used *SPAdes* v.3.12.0 (Bankevich et al., 2012) to assemble the cleaned reads into contigs and scaffolds. We then followed the single nucleotide polymorphism (SNP) calling pipeline used by McCormack et al. (2016). Briefly, we used *phyluce* (Faircloth, 2016) to match the assembled contigs to the probe set and determine how many loci were successfully assembled in each sample. We then built a probe

Table 1. Specimens used for linked genomic and phenotypic analysis.

Museum	Catalog	Location	Site	Lat	Lon
MLZ	26980	1 mi N Tapalpa, Jalisco, Mexico	1	19.960772	-103.75855
MLZ	26978	1 mi N Tapalpa, Jalisco, Mexico	1	19.960772	-103.75855
MLZ	26984	1 mi N Tapalpa, Jalisco, Mexico	1	19.960772	-103.75855
MLZ	26979	1 mi N Tapalpa, Jalisco, Mexico	1	19.960772	-103.75855
MVZ	122223	4 mi S Mazamitla, Jalisco, Mexico	2	19.8573541	-103.01944
MVZ	122216	4 mi S Mazamitla, Jalisco, Mexico	2	19.8573541	-103.01944
MVZ	122217	4 mi S Mazamitla, Jalisco, Mexico	2	19.8573541	-103.01944
MVZ	122219	4 mi S Mazamitla, Jalisco, Mexico	2	19.8573541	-103.01944
MLZ	24113	Rancho La Cofradia: 4 mi E Uruapán, Michoacán, Mexico	3	19.431778	-102.01743
MLZ	24115	Rancho La Cofradia: 4 mi E Uruapán, Michoacán, Mexico	3	19.431778	-102.01743
MLZ	24116	Rancho La Cofradia: 4 mi E Uruapán, Michoacán, Mexico	3	19.431778	-102.01743
MLZ	24118	Rancho La Cofradia: 4 mi E Uruapán, Michoacán, Mexico	3	19.431778	-102.01743
MLZ	55360	Lagunita, 13 mi NE Ario de Rosales, Michoacán, Mexico	4	19.35558	-101.67106
MLZ	55363	Lagunita, 13 mi NE Ario de Rosales, Michoacán, Mexico	4	19.35558	-101.67106
MLZ	55366	Lagunita, 13 mi NE Ario de Rosales, Michoacán, Mexico	4	19.35558	-101.67106
MLZ	55361	Lagunita, 13 mi NE Ario de Rosales, Michoacán, Mexico	4	19.35558	-101.67106
MLZ	57701	Puerto Morillos: 37 mi E Morelia by road, Michoacán, Mexico	5	19.66662	-100.80694
MLZ	57703	Puerto Morillos: 37 mi E Morelia by road, Michoacán, Mexico	5	19.66662	-100.80694
MLZ	57719	Puerto Morillos: 37 mi E Morelia by road, Michoacán, Mexico	5	19.66662	-100.80694
MLZ	57707	Puerto Morillos: 37 mi E Morelia by road, Michoacán, Mexico	5	19.66662	-100.80694
MLZ	30405	Puerto Lengua de Vaca, 15 mi E Zitacuaro, Mexico, Mexico	6	19.435109	-100.18668
MLZ	30413	Puerto Lengua de Vaca, 15 mi E Zitacuaro, Mexico, Mexico	6	19.435109	-100.18668
MLZ	30415	Puerto Lengua de Vaca, 15 mi E Zitacuaro, Mexico, Mexico	6	19.435109	-100.18668
MLZ	30408	Puerto Lengua de Vaca, 15 mi E Zitacuaro, Mexico, Mexico	6	19.435109	-100.18668
MLZ	41012	5 mi E Lerma, Mexico, Mexico	7	19.289842	-99.435342
MLZ	41050	5 mi E Lerma, Mexico, Mexico	7	19.289842	-99.435342
MLZ	41271	5 mi E Lerma, Mexico, Mexico	7	19.289842	-99.435342
MLZ	41051	5 mi E Lerma, Mexico, Mexico	7	19.289842	-99.435342
MLZ	23076	El Venerable, 4 mi E Río Frío, Puebla, Mexico	8	19.352327	-98.608858
MLZ	23077	El Venerable, 4 mi E Río Frío, Puebla, Mexico	8	19.352327	-98.608858
MLZ	46829	El Venerable, 4 mi E Río Frío, Puebla, Mexico	8	19.352327	-98.608858
MLZ	46851	El Venerable, 4 mi E Río Frío, Puebla, Mexico	8	19.352327	-98.608858

MLZ = Moore Laboratory of Zoology, Occidental College; MVZ = Museum of Vertebrate Zoology, University of California, Berkeley.

match database and a consensus fasta file for the sample with the greatest number of assembled loci, to serve as a pseudo-reference genome for mapping and calling SNPs for all samples. This was sample MVZ:Bird:122216, from which we recovered 4,756 UCE loci (mean among all samples = 4,480; range = 3,954–4,756). The mean UCE contig length for this pseudo-reference genome was 356 base pairs (bp), with a range of 175–3,250 bp. We used *bwa* v.0.7.15 (Li & Durbin, 2009) to map cleaned reads for each sample to this pseudo-reference genome, and converted the resulting SAM files to sorted BAM files using *SAMtools* v.1.3.1 (Li et al., 2009). We then removed PCR duplicates using *Picard* v.2.20.4 (distributed with *phyluce*; Broad Institute, 2019) and realigned each BAM file using *Genome Analysis Tool Kit* (*GATK*) v.3.8.1 (McKenna et al., 2010). We used *GATK* to call haplotypes from each BAM file as a gvcf file and then genotyped each sample, outputting a single multi-sample gvcf file. We extracted SNPs from this file, outputting a variant call format (vcf) file, removing SNPs with the following parameters: <5 bps from any insertion or deletion, found in a cluster of three or more SNPs within a 10 base pair window, SNP quality score <30, SNP quality score divided by allele depth (QD) <5, or strand bias >60.

We further filtered the resulting SNP dataset with a series of quality metrics using a custom filtering and visualization pipeline built using the R packages *SNPfiltR* (DeRaad, 2022) and *vcfR* (Knaus & Grünwald, 2017). These filters included removing all SNPs with more than two alleles, coding all heterozygous genotypes falling outside of a 0.25–0.75 allele balance range as missing, and removing all SNPs with a mean depth of coverage >100 (potential paralogs), in accordance with best practices for filtering reduced representation genomic datasets (O'Leary et al., 2018). We also visualized sample clustering across a suite of possible missing data thresholds to ensure that patterns of missing data were not driving patterns of sample clustering. Based on these exploratory analyses, we implemented an optimized per-SNP completeness threshold of 75%. We also implemented a minor allele count (MAC) cutoff across the entire dataset, removing singletons (MAC < 2) which are more likely to result from

sequencing error or DNA damage in historical samples. Post-filtering, we retained 5,028 high-quality SNPs shared across 2,669 UCE loci.

While attempting to identify fixed differences between the parental species, we discovered a putative UCE locus that contained 12 fixed differences between the parental species (populations 1 and 8). Using NCBI BLAST (Johnson et al., 2008), the probe sequence for this UCE locus (locus 5216 from the UCE 5K probe set) maps with the highest likelihood to chromosome 4 of the *Taeniopygia guttata* reference genome (98% coverage and 97.46% sequence identity). Yet the reference contig we assembled from this probe maps with the highest likelihood to the mitochondrial scaffold of the *T. guttata* reference genome (85% coverage and 88.6% sequence identity). This contig may reflect a structural rearrangement within the *Pipilo* lineage, but without a high-quality, in-group reference genome, we were unable to rule out mis-assembly. We, therefore, removed all SNPs mapping to this locus from downstream analyses, resulting in a complete dataset of 5,004 SNPs shared across 32 samples, with 2.6% overall missing data, and no individual sample missing genotype calls at >6% of the retained SNPs. After linkage filtering to only a single randomly selected SNP per UCE locus, we retained a filtered, unlinked dataset containing 2,668 SNPs with 2.9% overall missing data. We subsequently BLASTed each remaining UCE locus with a fixed SNP against the *T. guttata* reference genome, to ensure that none of the nuclear fixed differences we identified between the two species came from the mitochondrial genome.

To call mtDNA haplotypes, we assembled mitochondrial genomes from bycatch in our raw UCE sequence data by mapping to a publicly available *P. maculatus* mitochondrial genome (Genbank accession: FJ236291.1) using *MITObim* v.1.9.1 (Hahn et al., 2013). We manually extracted the ND2 gene from the mitochondrial reference genome and aligned each mitogenome to the reference ND2 sequence using *Geneious* v.8.9.1 (Kearse et al., 2012). We also used *Geneious* to manually recode obvious signs of mis-assembly or sequence error (e.g., spurious SNPs before and after sequence gaps) as missing, calculate an uncorrected ND2 pairwise distance matrix, and export the ND2 alignment as a nexus file. This nexus file was used as input for *PopART* v.1.7 (Leigh & Bryant, 2015), where we constructed a Median Joining Network, and color coded each haplotype based on sampling locality.

Genomic ancestry assignment

We used *ADMIXTURE* v.1.3.0 (Alexander et al., 2009) to assign each individual proportionally into a predefined number of genomic clusters, using the filtered, unlinked set of 2,668 SNPs as input. We performed replicate runs varying the number of clusters (K) from one to five and performing fivefold cross-validation. We removed rare alleles, which are known to affect inferences of population structure (Linck & Battey, 2019), by iteratively increasing the minor-allele count threshold required for an SNP to be included until cross-validation analysis indicated that the optimal clustering scheme switched from $K = 1$ to $K = 2$ (here, MAC ≥ 10; 229 retained SNPs). We retained ancestry scores (Q scores) for each individual for downstream analysis.

Cline analysis

We used the R package *HZAR* (Derryberry et al., 2014) to fit sigmoidal clines for each plumage trait, average phenotype score (across all six scored traits), genome-wide genetic ancestry (Q score), and mtDNA haplotype assignment for data from historical specimens. The modern comparisons were drawn from specimens collected between 2008 and 2009 (Kingston et al., 2014; Kingston et al., 2017). We generated a single set of geographic transect distances by recording, for both our historical transect and the modern transect collected by Kingston et al. (2014), the exact distance to the point nearest each sampling locality along a 688-km straight line between the westernmost and easternmost sampling localities (TV01 & TV08; Kingston et al., 2014). For each trait, we fit three nested, commonly implemented sigmoidal cline models (Barton & Hewitt, 1985; Brumfield et al., 2001) as in Royer et al. (2020), including a two-parameter model (cline center and cline width), a four-parameter model (cline center and width plus minimum and maximum values estimated), and a six-parameter model (cline center and width, minimum and maximum values, plus the shape of each tail estimated). Each model was fit using Markov Chain Monte Carlo (MCMC) with a length of 1M iterations, sampling from the posterior distribution every 100 iterations. We visualized the chain for each parameter and each model to ensure that parameter estimates achieved stationarity and retained the overall best-fit model based on the lowest AIC score. We then plotted the best-fit cline on top of the empirically observed mean population values for each trait and visualized the center of the cline for each trait and its upper and lower 2-log likelihood bounds.

Genotype-phenotype analysis

To assess the strength of the association between genotype and phenotype across this transect, we used R to plot the genome-wide ancestry score of each sample against individual trait values and calculate the sum of squared errors (SSE), or the sum of squared residuals from a 1:1 prediction line, where the given trait is perfectly predictive of the genomic ancestry of the sample. We used this approach to quantify the power of sampling locality and plumage to predict genomic ancestry at the level of individual birds.

Population genetics

We inferred an unrooted phylogenetic network by first calculating a pairwise genetic distance (Nei's D; (Nei, 1972)) matrix between all samples using the R package *StAMPP*. We then used this matrix as input for *SplitsTree4* v4.15.1 (Huson & Bryant, 2006) to build a Neighbor-Net, which effectively visualizes the genetic distance between individual samples, and can reveal conflicting data patterns that are not detectable under traditional phylogenetic inference (Bryant & Moulton, 2004).

We performed a principal component analysis (PCA) on the filtered 5,004 SNP dataset using the R package *adegenet* (Jombart, 2008). We identified SNPs fixed for alternate alleles between the two parental species (populations 1 and 8) using R (R Core Team, 2019). Because only eight out of 5,004 filtered, UCE-derived SNPs were fixed differences between parentals, we relaxed this threshold to a frequency difference of >0.8. We then used the 23 pseudodiagnostic SNPs as input for the R package *Introgress* (Gompert & Buerkle, 2010) to calculate a hybrid index and interspecific heterozygosity and plotted these values as a triangle plot using the R package *ggplot2* (Wickham, 2016). We note that our relatively small sample size from each parental population (four individuals, eight alleles)

is likely inflating the number of identified pseudodiagnostic SNPs, further underscoring the genomic homogeneity of the entire sampling transect. Additionally, we used the R package *StAMPP* (Pembleton et al., 2013) to calculate pairwise F_{ST} between sampling localities and plot pairwise F_{ST} along with pairwise fixed differences on a heatmap using *ggplot2*.

We used the R package *rEEMSplots* (Petkova et al., 2016) to calculate the estimated effective migration surface (EEMS) across the TMVB. We performed three replicate EEMS iterations each time using our filtered 5,004 UCE-derived SNP dataset as input, and varying the specified value for the parameter "nDemes" across the values 100, 200, and 400. We then visualized each EEMS iteration using *rEEMSplots*. After visually determining that the number of specified demes (nDemes) was not affecting the resulting migration surfaces, we chose to present the simplest iteration (nDemes = 100). We also used *rEEMSplots* to generate a scatterplot showing the relationship between geographic and genetic distance for all pairwise comparisons among sampling sites.

We used *pixy* v.1.2.6 (Korunes & Samuk, 2021) to calculate nucleotide diversity (Pi) of each sampling locality in sliding windows from an all-sites vcf file, which incorporates information from invariant sites. Incorporating invariant sites allows for a more accurate estimation of Pi that is more robust to missing data and more comparable across sequencing approaches. We followed *pixy* best practices for calculating genome-wide Pi by summing the pairwise genotype differences and dividing that by the sum of count comparisons for each sampling locality. We then calculated the proportion of heterozygous sites across all 5,004 filtered SNPs (i.e., heterozygosity) in each sample using R. We plotted heterozygosity per sample and Pi per sampling locality together on a single dot chart using *ggplot2*.

We used R to classify each of the 5,004 filtered nuclear SNPs into three classes—fixed, private, and shared—for each of the three identified lineages (populations 1 and 2, populations 3 and 4, and populations 5–8). We classified an SNP as fixed if a single allele was homozygous in all individuals and the allele did not occur in any other lineage. We classified an SNP as private if the lineage possessed a unique allele, but also shared the alternate allele with other lineages at a frequency >0. Finally, we classified an SNP as shared if both alleles present in the lineage also occurred in another lineage. We visualized these three classes of SNPs as bar charts for each sampling locality using *ggplot2*.

Species tree reconstruction

To reconstruct a species tree using sampling localities as tips, we used *SNAPP* implemented via *BEAST2* v2.6.4 (Bouckaert et al., 2014), using our 2,668 unlinked SNP dataset as input. For each replicate, we randomly downsampled each sampling locality to a single sample and ran an MCMC chain with length 5M, discarding the first 500K iterations as burn-in, and storing every 1,000th iteration. Using *Tracer* (Rambaut et al., 2018), we found that only one of our three replicates was able to achieve stationarity and an effective sample size >200 for all estimated parameters, so only the results from this replicate are presented here. We visualized all post-burn-in trees from the posterior distribution of this replicate on a single background using *DensiTree* (Bouckaert et al., 2014).

Demographic modeling

We used the R package *delimitR* (Smith & Carstens, 2020), a wrapper for *fastsimcoal2* v26 (Excoffier et al., 2021), to compare how well a series of demographic models could describe the evolutionary history of these populations. We used *easySFS* (github.com/isaacovercast/easySFS) to build a multispecies site frequency spectrum (mSFS) from our unlinked SNP dataset containing 2,668 UCE-derived SNPs, while assigning samples to three lineages from the *SNAPP* tree and PCA (sampling localities 1 and 2, 3 and 4, and 5–8). We used *fastsimcoal2* to simulate 10K replicates each for 10 possible demographic models including up to three distinct species and up to two instances of secondary contact, with sampling localities assigned to the following prespecified guide tree based on the species tree reconstructions: ((1–2, 3–4) 5–8). Because of our limited knowledge of the specific demographic histories of these populations, we roughly followed the default wide and flat priors for these simulations to minimize the effects of model misspecification. Specifically, we set a population size prior for each species at 10K–1M, a divergence time prior at 10K–100K generations for the first divergence and 100K–500K for the second divergence, and a prior on the proportion of individuals migrating between species under a migration model at 0.005–0.000005. We then converted our mSFS into a binned SFS specifying six distinct allele frequency classes and built a random forest (RF) classifier with 5K individual decision trees using the R package *abcrf* (Pudlo et al., 2016). We calculated the out-of-bag error rate for our RF classifier to quantify our power to discriminate among the 10 simulated demographic models, and finally had each of the 5K individual decision trees of the RF classifier vote for which simulated model was most likely to have produced our empirical SFS.

Environmental associations

We downloaded all iNaturalist records of *Pipilo* in the TMVB and filtered for research-grade observations without location masking. We manually clumped these records around the eight locations from the historical transect. For each GPS location, we extracted environmental data from the 19 WorldClim layers describing temperature and rainfall, as well as elevation and five habitat variables: canopy height, qscat (a measure of surface roughness), tree cover (%), NDVI (greenness), and standard deviation of NDVI (greenness seasonality). We conducted PCA to reduce the dimensionality of the data and explored environmental variation across the transect sites.

Results

Mitochondrial and genomic ancestry

An alignment of the mtDNA gene ND2 revealed two highly divergent mitochondrial haplotypes separated by 4.8% uncorrected *p*-distance, corresponding to the two parental species (Figure 1B). Parental haplotypes were mostly fixed between populations 1 and 2 and 3–8, except for one Spotted Towhee haplotype found in population 2.

ADMIXTURE analyses revealed that when low-frequency variants are removed (SNPs with MAC <10), the optimal number of genetic clusters is $K = 2$, with genomic ancestry (Q score) changing gradually along the transect and individuals within a site having similar ancestry prediction (Figure 1C). Under $K = 3$, six of eight individuals at sites 3 and 4 in the middle of the transect show greater than 50% assignment to a distinct third cluster, with three of these individuals having 100% assignment to this cluster.

Cline analysis

The plumage scores of 32 genomics-associated historical specimens were broadly representative of a larger sample of 73 historical specimens collected from the same sites (Supplementary Table S1). Cline centers for autosomal genomic ancestry and overall plumage score occurred in the center of the transect between populations 4 and 5, significantly offset from the mtDNA cline center, which was located about 250 km to the west, closer to the Collared Towhee side (Figure 2A). When plumage traits were disaggregated, individual traits showed significant variation in their cline centers (Figure 2B). Throat color aligned with the west-shifted cline center for mtDNA, whereas back color, back spots, and tail spots were shifted about 100 km east of the average phenotypic cline center. Meanwhile, flank color and pileum (brown cap) found their cline centers near the population averages. Cline centers were consistently stable over a 70-year period, with all measured traits displaying overlapping 2 log-likelihood ranges when comparing the historical and modern transects (Figure 2).

Phenotype-genotype associations

In addition to comparing clines at the level of the whole gradient, we also analyzed the strength of the association between phenotype and genotype at the level of the individual bird. Location on the transect is more tightly correlated with genomic ancestry than any phenotypic measurement (SSE = 0.67, Figure 3). Additionally, the average phenotype (the score for all six plumage characteristics summed) is more tightly correlated with the genomic ancestry of a given sample (SSE = 0.99) than any individual plumage trait (min SSE = 1.43). Both back color (SSE = 5.55) and throat color (SSE = 4.04) stand out for being highly decoupled from the genomic ancestry of individual birds throughout the transect.

Population genetics

To better understand the population dynamics within the hybrid zone, we employed a suite of descriptive population genetic approaches. A key revelation from plotting ancestry against heterozygosity was that, within the central populations (3 and 4), there are no parental types or recent backcrosses, but instead a homogenized population of genomically intermediate birds (Figure 4C). Additionally, a distance-based, unrooted phylogenetic network generated from all 5,004 nuclear-filtered SNPs supports three lineages, with the geographically intermediate lineage (populations 3 and 4) connecting populations 1 and 2 and populations 5–8 (Figure 4A). Despite short internal branches on this network, reflecting the low overall divergence, microgeographic structure is apparent among sampling localities, with individuals from nearly every sampling locality clustering together. Similarly, a PCA reveals three distinct genomic clusters, where populations 3 and 4 are again identified as intermediate, but discrete populations (Figure 4B). F_{ST} estimated between parental ends of this cline using all UCE-derived SNPs = 0.12, recapitulating the finding of limited differentiation across this cline by Kingston et al. (2017), who estimated F_{ST} = 0.101 between parental ends using thousands of GBS loci. F_{ST} estimates also reveal low overall levels of divergence between sampling sites (mean pairwise F_{ST} = 0.06), and nearly undetectable levels of differentiation between neighboring sampling localities (mean pairwise F_{ST} = 0.03; Figure 4D). Out of 5,004 UCE-derived SNPs, only eight are fixed for different alleles between the geographical extremes of the transect.

The estimated effective migration surface shows two distinct decreases in effective migration (i.e., gene flow) west of population 3 and east of population 4 (Figure 5A), despite identifying no significant deviations from an isolation-by-distance model (Figure 5B). This migration surface

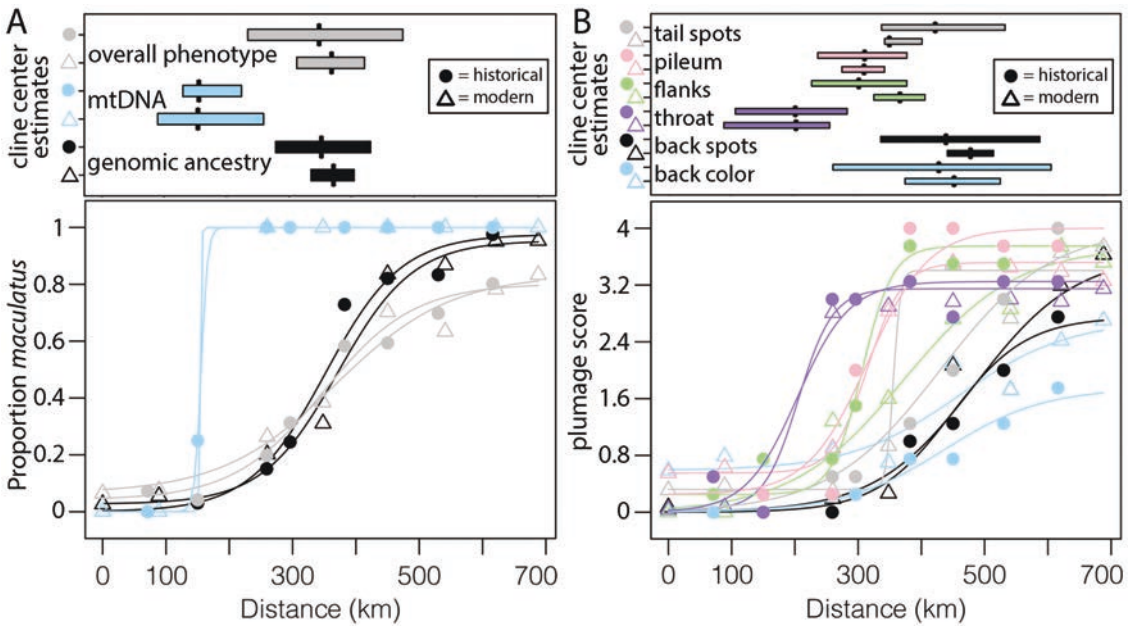

Figure 2. Geographic clines showing the transition of (A) genetic and (B) phenotypic characters across the TMVB gradient. Barplots above each cline correspond to the cline center estimate for the given trait, with a black vertical dash indicating the point estimate, and the extent of the colored bar illustrating the two log-likelihood confidence interval. The mean value of each modeled trait for each sampling locality is shown with a corresponding color-coded shape icon.

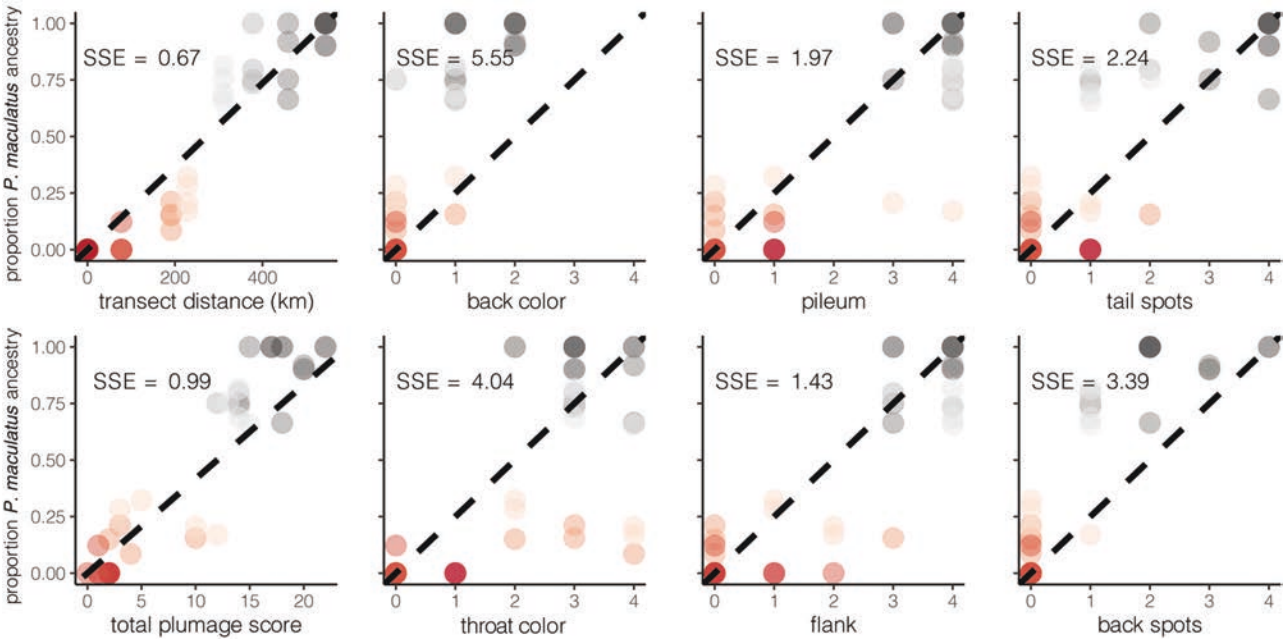

Figure 3. Scatter plots showing genotype-phenotype correlations for 32 historic *Pipilo* specimens across the TMVB with linked genetic and trait data. For each plot, the y-axis is the proportion of genomic ancestry assigned to *P. maculatus* for a given individual under a $k = 2$ model. The sum of squared errors (SSE), or the sum of all squared residual distances from the expected 1:1 line (dashed line), quantifies the predictive accuracy of the given independent variable. Correlations are shown for six divergent plumage characteristics, which are scored on a 0–4 scale, where 0 indicates pure *ocai* phenotype and 4 indicates pure *maculatus* phenotype, Sibley (1950). Each sample is color coded according to sampling locality, matching the color scheme from Figure 1.

also revealed a slight increase in effective migration rate among populations 5–8, which are located within a relatively continuous swath of suitable montane habitat. A linear regression shows that >80% of the variance in pairwise genetic dissimilarity between sampling localities can be explained by a positive, linear relationship with pairwise geographic distance (Figure 5B).

Contrary to the elevated heterozygosity expected in the middle of a cline under a two-species tension-zone model, we found little variation in heterozygosity and genetic diversity between sampling localities across the transect (Figure 5C). A visualization of the number of shared, private, and fixed alleles in each of the three genomically distinct populations reveals that nearly all SNP variation is shared between multiple populations along the transect, and there are no fixed variants between populations (Figure 5D). The presence of private alleles in the admixed population (sampling localities 3 and 4) may indicate a degree of genetic isolation, although this result must be interpreted with caution considering our limited sample size.

Phylogenetic analysis

The *SNAPP* species tree (Figure 6A) placed the eight sampling localities into three recently diverged lineages corresponding to the three discrete genomic clusters identified via population genetic approaches; sampling localities 1 and 2 (Collared Towhee), localities 5–8 (Spotted Towhee), and a third lineage, which is sister to Collared Towhee, made up of sampling localities 3 and 4 from the center of the transect. The 4,500 overlaid trees sampled from the posterior distribution of species trees reveal some uncertainty in the phylogenetic relationships among these three lineages.

Demographic modeling

The best-supported demographic model describing this sampling transect was a three-species model with multiple gene flow edges (Figure 6B), where each of the three lineages described above is assigned to a distinct species (posterior probability = 0.75). The high out-of-bag error rates (i.e., model misspecification rate in the training dataset) observed for many of the models we simulated indicates that we have limited power to discriminate between highly similar demographic scenarios, yet three-species models (with various degrees of gene flow) consistently outperformed one- or two-species models despite penalization of each additional parameter added beyond the one-species base model.

Niche analysis

Climate, habitat, and elevation data collected from around the sampling locations indicate niche differences along the gradient (Figure 7). Spotted Towhees in the eastern part of the gradient are at the highest average elevation, followed by Collared Towhees in the west. The center of the gradient, where most of the phenotypic and genetic transitions occur, is at the lowest elevation. PCA revealed several important axes of variation that explain climatic differences across the gradient (Supplementary Table S2). PC4, which describes differences in rainfall seasonality, showed a sharp transition within hybrid population 3, coinciding with cline centers in throat color and mtDNA. Individuals west of Mt. Tancítaro (populations 1, 2, and part of population 3) are found in habitats with a summer monsoon rainfall schedule and greater seasonality in rainfall and vegetation greenness.

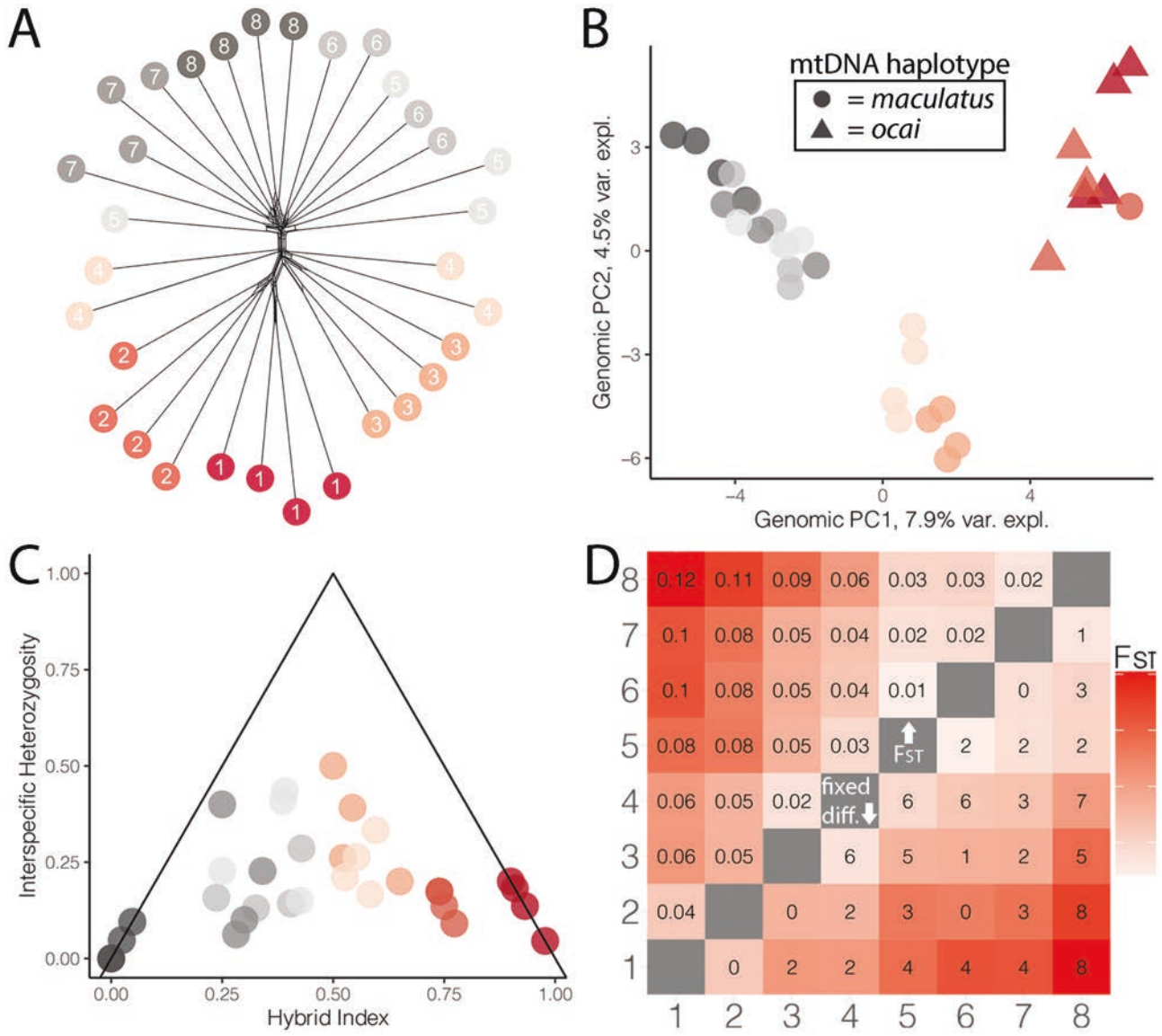

Figure 4. (A) An unrooted phylogenetic network constructed from a distance matrix using the 5,004 filtered, UCE-derived SNP genotypes as input. (B) PCA using all 5,004 filtered SNPs, with samples colored according to sampling locality. (C) Triangle plot showing hybrid index and interspecific heterozygosity calculated using 23 SNPs highly differentiated between sampling localities 1 and 8. (D) Heatmap depicting pairwise F_{ST} between all eight sampling localities above the diagonal, and the number of fixed differences for each pairwise comparison below the diagonal.

Discussion

> "I think that the most logical interpretation of this gradient population series is to consider it to represent an elongate hybrid zone, the geographically limited segments of which have attained a certain degree of stability and differ from one another by the same amount, as do typical geographic races of one species."
>
> Charles G. Sibley (1950)

Many hybrid zones have been described as tension zones, where pure parental species disperse along a unidirectional cline and hybridize in the center to form F1s, which are selected against (Slatkin, 1973; Barton & Hewitt, 1985). Our genetic results confirm that the classic hybrid zone between the Collared Towhee (*P. ocai*) and Spotted Towhee (*P. maculatus*) is not a tension zone. Instead, introgression across a broad area—what Sibley (1950) called an "elongate hybrid zone"—has erased nearly all fixed autosomal differences between the two ends of the cline. Only 8 of 5,000 autosomal SNPs are fixed (F_{ST} = 0.12). Meanwhile, mtDNA haplotypes for the two species differ at a median of 51 sites over 1,040 bp of *ND2* (Figure 1B), translating to 4.8% divergence—likely over two million years of evolutionary isolation before secondary contact. The towhee gradient, therefore, may be similar to some other hybridizing bird species where the genes controlling plumage differences account for much of the existing autosomal genomic differentiation (Poelstra et al., 2014; Toews et al., 2016; Wang et al., 2020).

Sibley (1950) speculated that contact between the two species might have been initiated by human-mediated habitat change in the TMVB, an area of significant human settlement since pre-Columbian times. Our historical comparison, however, shows that the hybrid zone has not changed substantially over the course of 70 years. There is remarkable concordance between historic and modern clines centers for phenotypic traits and genetic markers

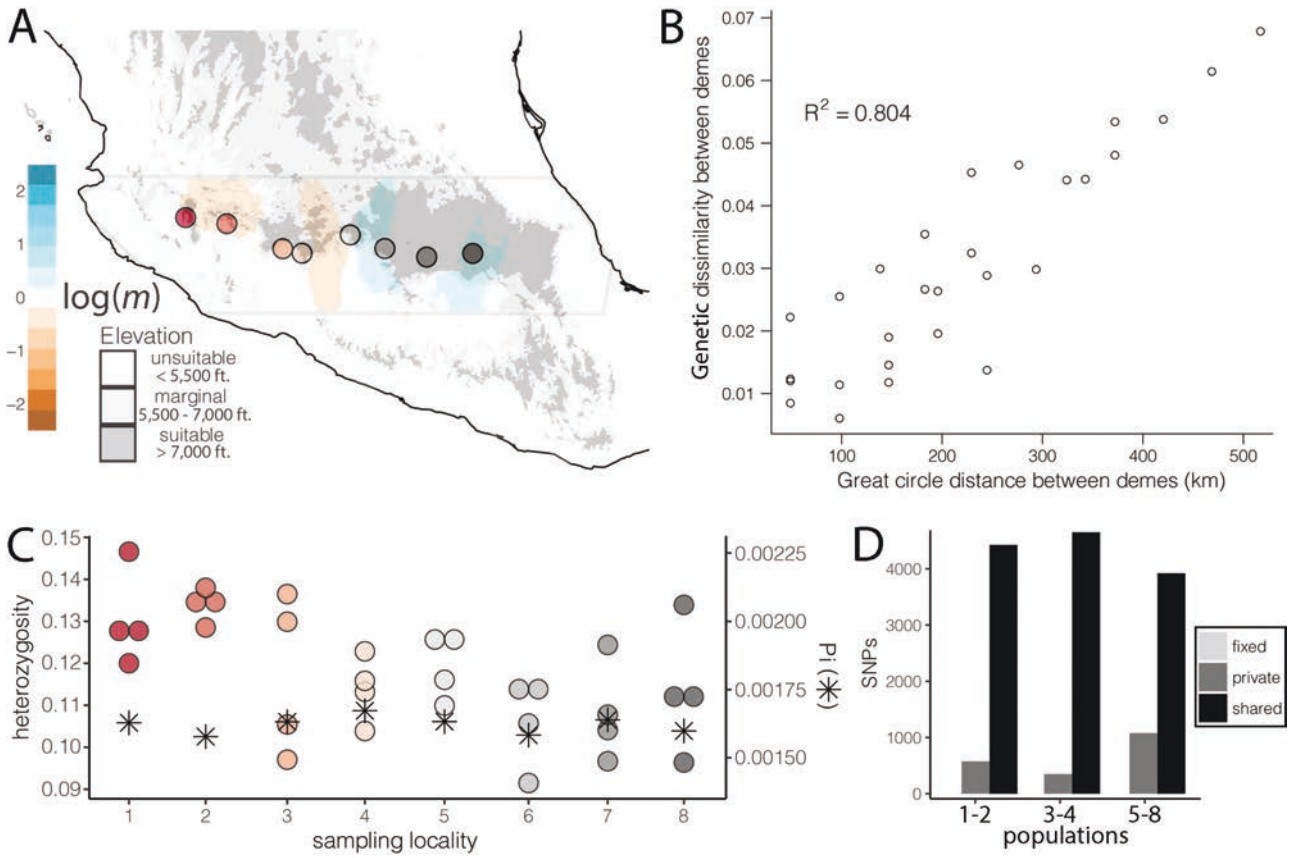

Figure 5. (A) Estimated effective migration surface plotted geographically, with shading indicating regions deviating from a null model of IBD (i.e., log(*m*) = 0). (B) Scatter plot between geographic and genetic distance for all pairwise comparisons between sampling localities. The R^2 value indicates the proportion of variation in genetic dissimilarity between sampling localities predicted by the geographic distance between sampling localities. (C) Heterozygosity of each individual and the nucleotide diversity (population-wide Pi value indicated by an asterisk) of each sampling locality. (D) Number of fixed, private, and shared alleles present in each of the three identified lineages from Figure 6.

(Figure 2), especially considering that the estimates stem largely from different specimens measured by different observers. Among the few studies that have assessed temporal change to hybrid zones using historical genomics of museum specimens, hybrid zone movement (Carling & Zuckerberg, 2011; Leaché et al., 2017; Ryan et al., 2018; Taylor et al., 2014) has been more commonly documented than stability (Wang et al., 2019). Buggs (2007) also outlined numerous case studies of hybrid zone movement over historical time periods. While it is possible that the towhee clines might have shifted at finer scales than our sampling was able to detect (our sites averaged 80 km apart), this is nonetheless significant stability for a region marked by human impacts and suggests this hybrid zone has broadly achieved an equilibrium state.

If secondary contact between these species is not recent, then it was likely brought about by habitat fluctuations during the Pleistocene or Holocene, perhaps as recently as 1,000 years before present (BP), which marks the last major climatic perturbation—a drying event that affected habitat across the TMVB (Metcalfe et al., 2000). Paleoecological data from the region, including a pollen core from the heart of the hybrid zone at Lake Patzcuaro, Michoacán, support the continuous and abundant presence of pine forest in the region dating back to 44,000 years BP (Watts & Bradbury, 1982). A synthetic review of the paleoclimate of the TMVB around the last glacial maximum (LGM) points to the expansion of a pine-fir assemblage to lower elevation (Caballero et al., 2010), meaning secondary contact could date to the LGM, if not before. Future investigations using whole-genome data could test these hypotheses by estimating the timing of initial contact using the size of recombination blocks in hybrid birds (Griffiths & Marjoram, 1996).

While the exact timing of secondary contact remains to be clarified, it seems plausible that, during the LGM, gene flow between Collared Towhees and Spotted Towhees was more extensive across the TMVB. During subsequent warming, montane forests moved upslope and shrunk, creating the current patchwork of sky-island forests (Caballero et al., 2010). In one of these forested sky islands in Michoacán, a hybrid lineage, including population samples 3 and 4, appears to have attained a degree of evolutionary isolation (Figures 4B and 6). Thus, while certain aspects of the towhee gradient can be understood and analyzed as a cline (Figure 2), it can also be described as an elongated region of continuous hybridization (Figure 5B), or as three recently diverged lineages with ongoing gene flow (Figure 6A). Beyond the question of how one might layer a taxonomy over this variation, which we discuss later, the towhee system represents an empirical example of the potential for hybrid zones, through vicariance, to spawn novel variation (Barton et al., 1983; Guiller et al., 1996; Soltis, 2013) and incipient lineages of hybrid origin (Hamilton et al., 2013; Lamichhaney et al., 2018; Seehausen, 2004).

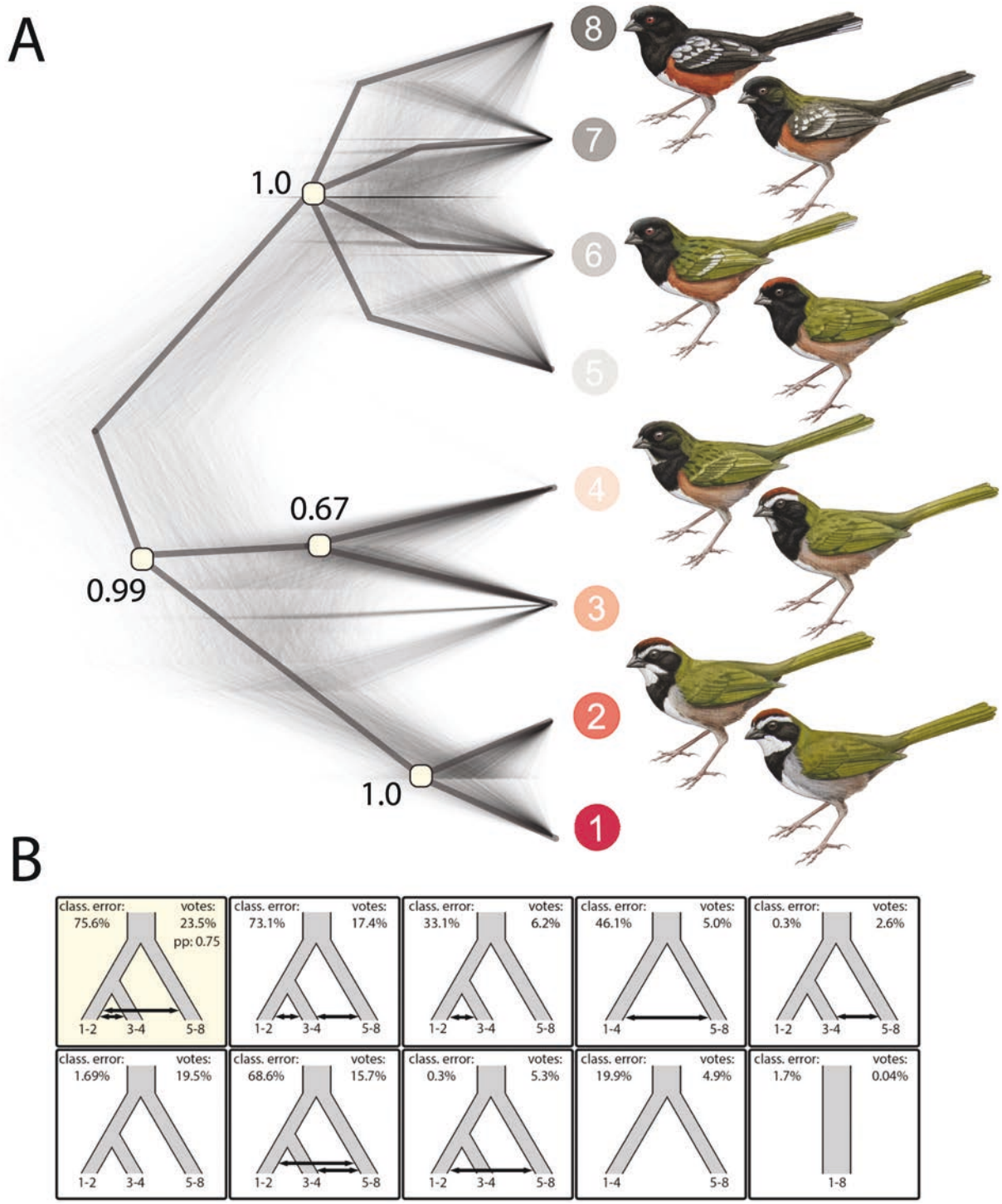

Figure 6. (A) Cloudogram of 4,500 trees sampled from the posterior distribution of species trees with posterior probabilities (pp) at each node. Nodes with less than 0.60 pp were collapsed. Towhee illustrations by Alex Warnick. (B) Relative support for each of the ten demographic models that were tested for their ability to describe the evolutionary history of *P. ocai* and *P. maculatus* populations along the TMVB. "Votes" indicates the percentage of random forest decision trees voting for a given model as most likely to have generated the observed data, while "class. error" indicates the classification error, i.e., frequency of misclassification of the given model under simulated conditions, and "pp" indicates the posterior probability of the most supported model.

Differential introgression: coincident clines in mtDNA and a putative sexual signal

One of the striking features of the towhee gradient is the difference in cline centers—i.e., cline shifts—across traits and markers. Cline shifts result from differential introgression of traits and genetic markers. Although cline shifts can result from genetic drift depending on the conditions (Polechová & Barton, 2011), they are predicted under natural selection and therefore provide a rationale for preliminary investigations of the potential adaptive significance of the introgressing traits (Hofman & Szymura, 2007; Jaarola et al., 1997; Lipshutz et al., 2019; Parsons et al., 1993). Across the towhee hybrid

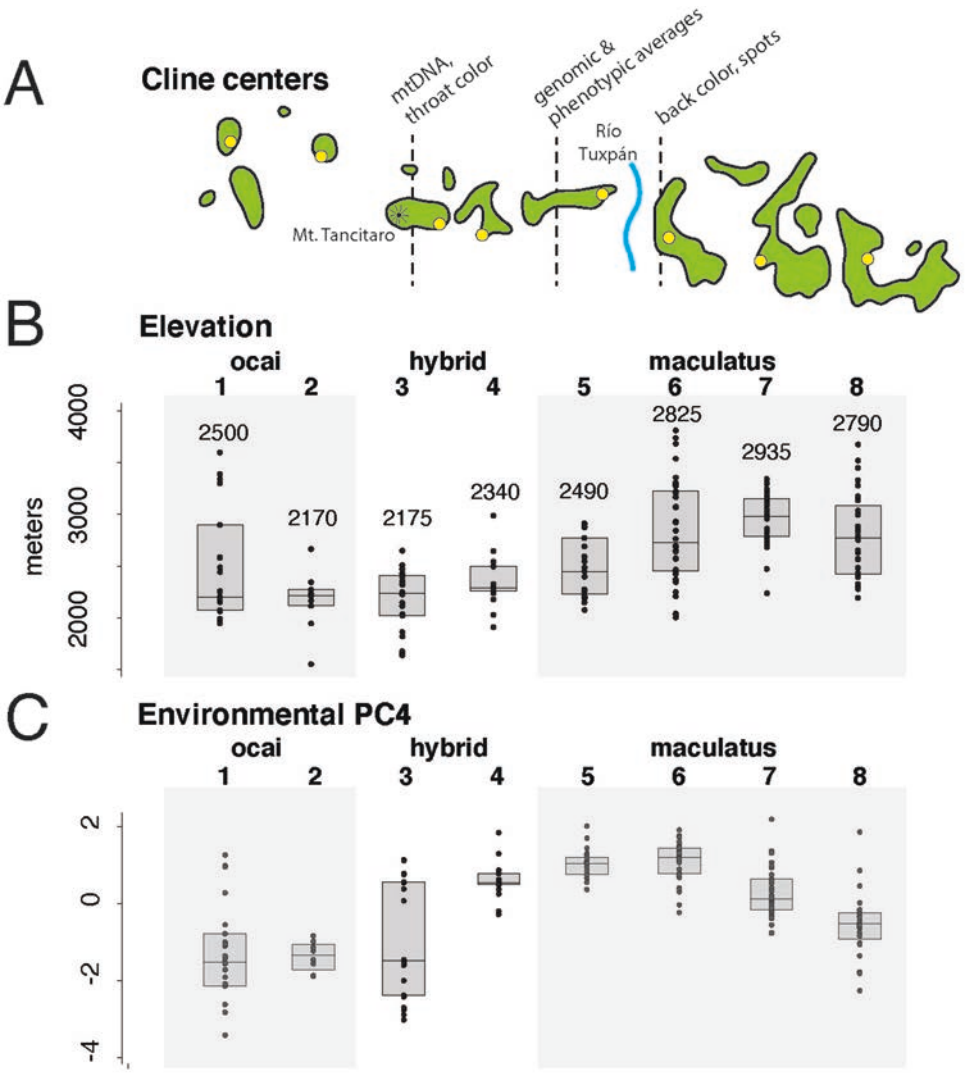

Figure 7. Niche results. (A) Forested landscape and summary results on cline centers from Figure 2. (B) Elevational variation with population means above each box and whisker plot. The hybrid lineage occurs at low elevation. *P. maculatus* is at a higher elevation than hybrid or *P. ocai* populations. (C) Environmental variation. Principal component 4 describes rainfall and greenness seasonality. There is a bimodal distribution in population 3 aligning with cline centers for mtDNA and throat color.

zone, when genomic markers and phenotypic traits are averaged, cline centers fall in the middle of the transect, between populations 4 and 5, coincident with the deepest split in the species tree. But these averages belie significant discordance among traits (Figure 2). The cline centers for throat color and mtDNA are shifted ~250 km west toward the Collared Towhee side of the cline and feature sharp transitions, suggesting selection against hybrids. Another group of traits—back color, back spotting, and tail spotting—are shifted ~100 km east toward the Spotted Towhee side of the gradient. Meanwhile, cap color (pileum) and flank color find their cline centers near the averages for total plumage score and genomic ancestry. These population-level patterns are recapitulated at the level of the individual, where linked genetic and phenotypic data show that an individual's throat color and back color are poor predictors of genomic ancestry (Figure 3).

Cline shifts seem especially common in sexually-selected signals (Baldassarre et al., 2014; While et al., 2015) or dominance-associated traits (Lipshutz et al., 2019), and the strongly-shifted and coincident clines between throat color and mtDNA could suggest a common mechanism. Both cline centers fall just west of population 3, meaning that the break occurs between the Collared Towhee lineage and the hybrid lineage. This pattern supports two possibilities involving sexual selection. The mitonuclear incompatibility hypothesis for sexual selection by female choice posits that females use plumage as a proxy for mitonuclear compatibility (Hill & Johnson, 2013), providing a potential mechanism for linked introgression of plumage traits and mtDNA. Even without mitonuclear compatibility, however, if female Collared Towhees prefer white-throated males, then selection against hybrid throat types would create a narrow cline in throat color, which would become linked to the mtDNA cline due to the matrilineal inheritance of mtDNA. Haldane's Rule has been proposed as a possible mechanism for narrow cline widths in mtDNA compared to other markers in birds (Carling & Brumfield, 2008; Gowen et al., 2014), but is a less compelling explanation here because of the general lack of postmating isolation. Genetic drift should not be ruled out, however, as clines can shift stochastically with low population sizes (Barton, 1979), especially if the cline is old (Jofre & Rosenthal, 2021) or occurs across a patchy landscape (Sequeira et al., 2022).

In other systems with clines shifts in sexually-selected traits, field studies have confirmed the universal female preference for one trait (Baldassarre & Webster, 2013; McDonald et al., 2001; Stein & Uy, 2006), leading to unidirectional introgression (Baldassarre et al., 2014; Brumfield et al., 2001). However, this might not be the case in the towhee system. Assortative mating for throat color is a possibility, and white throats might also be better seen and therefore adaptive in the low-light micro-niches favored by Collared Towhees. Field studies of mate preferences could help clarify whether the sexual selection is acting on throat color. Additionally, whole-genome analysis could help test for the role of drift and identify the loci involved in throat color and whether they show signatures of selection or mitonuclear associations (e.g., Wang et al., 2021a).

Green back color presents another potentially adaptive cline shift, albeit in the opposite direction, this time of a Collared Towhee trait introgressing far into the phenotypic background of Spotted Towhees. In fact, back color never reaches its full parental black Spotted Towhee appearance even at the far eastern end of our sampled cline. Could green back color be adaptive for camouflage? This hypothesis is difficult to test absent field studies. However, it has been noted that the TMVB Spotted Towhees occur in fir forest at significantly higher elevation compared to conspecific populations throughout the rest of the species range (Rising, 2020)—habitat that is typically more associated with Collared Towhees. The elevational differences across the gradient are likewise intriguing (Figure 7B), with the Spotted Towhee side of the gradient at a higher elevation than the Collared Towhee side, and the hybrid lineage at the lowest elevation. Future investigations into the specific genes encoding traits like back color and associations with elevation, as well as specific tests for the roles of selection and drift, will be crucial to testing adaptive introgression in this system (e.g., Kozak et al., 2021).

A hidden environmental break marks a key transition in genetics and phenotype

> "Only 50 miles west of Patzcuaro, without an intervening barrier, the Tancítaro and Patambán birds show a still closer approach to *ocai*...."
>
> Sibley (1950)

The formation of hybrid zones can occur due to rapid environmental transitions that bring two species into close proximity (Endler, 1977), or they might trace back to expansions from glacial refugia (Swenson & Howard, 2005), with the hybrid zone forming wherever the expanding range margins happen to meet and then moving based on additional factors. In the towhees, habitat variation had not been carefully studied to understand whether clinal transitions in traits or genes are associated with environmental turnover. Sibley described some habitat differences across the gradient, but also placed emphasis on geographic barriers, like the Río Tuxpan. He puzzled over the transition of phenotypes in the western part of the gradient, near the hybrid lineage, where there were no obvious vicariance barriers. Kingston et al. (2014) created a connectivity map that suggested habitat connections in the eastern part of the gradient (populations 5–8), and more patchiness in the center of the gradient around the hybrid lineage, both patterns supported by our genomic results. However, this analysis was based on holistic climate-based niche models, and it was not clear which climate variables or habitat features might be driving the patterns.

Our transect approach to assessing environmental change uncovered a major, and previously overlooked, environmental transition in western Michoacán, which coincides with turnover in throat color and mtDNA (Figure 7). From Mount Tancítaro to the west, core Collared Towhee habitat has a heavy summer rainfall schedule and less variation in vegetation greenness. This transition, and especially the marked influence of Mount Tancítaro, western Mexico's second highest peak, on the climate of the region and its rainfall, has been noted in older botanical works (Leavenworth, 1946), but has not been associated with animal niches to our knowledge.

What influence these environmental features might have on the towhees is not clear, but rainfall schedules could influence the time of breeding, with temporal mismatch acting as a barrier to gene flow. Population 3, lying close to sharp transitions in throat color, mtDNA, and this niche axis, likely holds many clues to understanding the towhee gradient (Figure 7C). Importantly, turnover in traits and markers can become associated with environmental barriers without the barriers necessarily being the cause of initial divergence (Bierne et al., 2011). More fine-scale sampling across this environmental break, combined with quantitative associations between environmental characteristics and genomic markers (e.g., Alvarado et al., 2022), could help test for a causative role of ecological factors in the formation and maintenance of the gradient.

Hybrid zone or hybrid lineage?

While our results provide the most comprehensive systematic data set collected to date in this system, we echo more than 70 years of research indicating that this system presents a particularly challenging situation for Linnean taxonomy. If there is a species-level break in the gradient, our genomic results support Sibley's original assessment that it is best located between populations 4 and 5, with populations to the east (5–8) considered Spotted Towhees, though marked by introgression. The Olive-backed Towhee recognized by some authorities can be aligned with these populations (5–8) and the subspecies *P. m. macronyx*. The bigger taxonomic question involves the hybrid lineage formed by populations 3 and 4. This lineage has Spotted Towhee mtDNA, but is closer to Collared Towhee in autosomal ancestry. Given present knowledge, we would call these populations hybrids or assign them to Collared Towhee, matching the dominant genomic ancestry and the majority of phenotypic traits. The black throat color of this hybrid lineage, matching the Spotted Towhee, could be governed by a single locus (as in the ASIP gene in *Vermivora* warblers; Baiz et al., 2020), and the Spotted Towhee mtDNA haplotype, inherited as a single locus, could be subject to stochastic events (Ballard & Whitlock, 2004). It is humbling to recognize that many of the novel genomic patterns we document here simply bear out Sibley's (1950) taxonomic recommendations, which he seemed to dismiss as a mere "nomenclatural convenience," following decades of careful field observations and study of museum specimens.

Beyond taxonomy is the equally difficult-to-resolve question of the evolutionary history and trajectory of this towhee gradient. One of the more striking conclusions of our study is how the gradient can be simultaneously interpreted under a one-population isolation-by-distance model, a two-population classical hybrid zone model, and a three-lineage model with gene flow,

underscoring the continuum between clinal variation across a hybrid zone and hybrid lineage formation (Ottenburghs, 2018)—and perhaps eventual hybrid speciation (Nieto Feliner et al., 2020), although this would require the establishment of reproductive barriers. Hybrid speciation is debated, with some reserving the term for allopolyploid hybrid speciation, where hybridization triggers instantaneous reproductive isolation in daughter lineages (Grant, 1981; Schumer et al., 2014). To use the term hybrid speciation here requires the inclusion of homoploid hybrid speciation events, where a lineage of hybrid origin gradually evolves reproductive isolating mechanisms from parental species following an initial admixture pulse (Abbott et al., 2013; Mallet, 2007; Feliner et al., 2017).

While the hybrid lineage we identified currently meets few of the criteria required for species recognition, the situation of an elongated hybrid zone and vicariance offers the potential for future hybrid speciation under natural conditions. At the very least, the hybrid lineage contains novel phenotypic combinations and unique genetic variants, adding to results from other studies that hybrid populations can harbor evolutionary novelty (Barton et al., 1983; Schilthuizen & Gittenberger, 1994). If homoploid hybrid speciation can proceed in sympatry (Olave et al., 2022), then allopatric cases must be even more common, yet they have rarely been documented. An allopatric mode of homoploid hybrid speciation may be overlooked in contemporary genomic research because complex biogeographic scenarios are difficult to reconstruct in hindsight compared to allopolyploid speciation events, which leave clear karyotypic and genomic signatures in daughter hybrid species (Barley et al., 2022), or sympatric cases, where the parental and daughter species are still living side-by-side. The towhee system offers a special opportunity to study how homoploid hybrid speciation might begin in nature, because rather than relying on the fraught process of historical biogeographic reconstruction, we are offered a chance to observe an incipient hybrid lineage evolving in relative geographic isolation in real-time.

As hybridization is studied in detail with phenotypic and genomic analysis, it has become clear that gene flow is both a ubiquitous and generative force in evolution (Jiggins et al., 2008; Lamichhaney et al., 2018; Selz & Seehausen, 2019; Wang et al., 2021b). Here, integrative data from genomics, phenotype, and environment show that Sibley's classic hybrid zone, in addition to generating a gradient of forms between two species, has also led to an isolated hybrid population. While cline analyses will continue to be useful for understanding hybrid zones, our study highlights the potential of admixture and directional introgression followed by vicariance to set the stage for the generation of novel forms. Increased genomic data, denser geographic sampling, and more sophisticated demographic analyses will continue to expand our understanding of the continuum between hybrid zones and hybrid lineages and the role hybridization plays in driving large-scale patterns of biodiversity.

Supplementary material

Supplementary material is available online at *Evolution* (https://academic.oup.com/evolut/qpac068)

Data availability

The raw data underlying this article are available in Dryad Digital Repository at https://doi.org/10.5061/dryad.59zw3r2c5. Raw sequence data is permanently archived via SRA at: https://www.ncbi.nlm.nih.gov/bioproject/915057. The scripts for analyzing genetic data and outputs are available in the Supplementary Material and are included in a publicly available, thoroughly documented GitHub repository (https://github.com/DevonDeRaad/towhees.uces). All code is permanently versioned and archived at: https://www.doi.org/10.5281/zenodo.7535580.

Author contributions

D.A.D. analyzed data, interpreted results, and co-wrote the paper; E.E.A. collected data and edited the paper; W.L.E.T. collected data and co-wrote the paper; R.S.T. analyzed results and edited the paper; S.E.K. collected data and co-wrote the paper; M.J.B. co-wrote the paper; J.E.M. collected data, analyzed results, and co-wrote the paper.

Conflict of interest: The authors declare no conflict of interest.

Acknowledgments

Access to specimen material was facilitated by UC Berkeley's Museum of Vertebrate Zoology (C. Cicero) and the Moore Laboratory of Zoology (J. Maley). Funding was provided by National Science Foundation grants DEB-1258205 and DEB-1652979 to J.E.M., the Borestone Fund, and the Occidental College Undergraduate Research Center.

References

Abbott, R., Albach, D., Ansell, S., Arntzen, J. W., Baird, S. J., Bierne, N., Boughman, J., Brelsford, A., Buerkle, C. A., Buggs, R., Butlin, R. K., Dieckmann, U., Eroukhmanoff, F., Grill, A., Cahan, S. H., Hermansen, J. S., Hewitt, G., Hudson, A. G., Jiggins, C., … Zinner, D. (2013). Hybridization and speciation. *Journal of Evolutionary Biology*, 26(2), 229–246. https://doi.org/10.1111/j.1420-9101.2012.02599.x

Alexander, D. H., Novembre, J., & Lange, K. (2009). Fast model-based estimation of ancestry in unrelated individuals. *Genome Research*, 19(9), 1655–1664. https://doi.org/10.1101/gr.094052.109

Alvarado, A. H., Bossu, C. M., Harrigan, R. J., Bay, R. A., Nelson, A. R., Smith, T. B., & Ruegg, K. C. (2022). Genotype-environment associations across spatial scales reveal the importance of putative adaptive genetic variation in divergence. *Evolutionary Applications*, 15, 1390–1407. https://doi.org/10.1111/eva.13444

Baiz, M. D., Kramer, G. R., Streby, H. M., Taylor, S. A., Lovette, I. J., & Toews, D. P. (2020). Genomic and plumage variation in *Vermivora* hybrids. *The Auk*, 137, ukaa027. https://doi.org/10.1093/auk/ukaa027

Baldassarre, D. T., & Webster, M. S. (2013). Experimental evidence that extra-pair mating drives asymmetrical introgression of a sexual trait. *Proceedings of the Royal Society B: Biological Sciences*, 280(1771), 20132175. https://doi.org/10.1098/rspb.2013.2175

Baldassarre, D. T., White, T. A., Karubian, J., & Webster, M. S. (2014). Genomic and morphological analysis of a semipermeable avian hybrid zone suggests asymmetrical introgression of a sexual signal. *Evolution*, 68(9), 2644–2657. https://doi.org/10.1111/evo.12457

Ballard, J. W. O., & Whitlock, M. C. (2004). The incomplete natural history of mitochondria. *Molecular Ecology*, 13(4), 729–744. https://doi.org/10.1046/j.1365-294x.2003.02063.x

Bankevich, A., Nurk, S., Antipov, D., Gurevich, A. A., Dvorkin, M., Kulikov, A. S., Lesin, V. M., Nikolenko, S. I., Pham, S., Prjibelski, A. D., Pyshkin, A. V., Sirotkin, A. V., Vyahhi, N., Tesler, G., Alekseyev, M. A., & Pevzner, P. A. (2012). SPAdes: A new genome assembly algorithm and its applications to single-cell sequencing. *Journal of*

Computational Biology, 19(5), 455–477. https://doi.org/10.1089/cmb.2012.0021
Barley, A. J., Nieto-Montes de Oca, A., Manríquez-Morán, N. L., & Thomson, R. C. (2022). The evolutionary network of whiptail lizards reveals predictable outcomes of hybridization. *Science*, 377(6607), 773–777. https://doi.org/10.1126/science.abn1593
Barton, N. H. (1979). The dynamics of hybrid zones. *Heredity*, 43(3), 341–359. https://doi.org/10.1038/hdy.1979.87
Barton, N. H., Halliday, R., & Hewitt, G. (1983). Rare electrophoretic variants in a hybrid zone. *Heredity*, 50, 139–146. https://doi.org/10.1038/hdy.1983.15
Barton, N. H., & Hewitt, G. M. (1985). Analysis of hybrid zones. *Annual Review of Ecology and Systematics*, 16, 113–148. https://doi.org/10.1146/annurev.es.16.110185.000553
Bennett, K. F., Lim, H. C., & Braun, M. J. (2021). Sexual selection and introgression in avian hybrid zones: Spotlight on *Manacus*. *Integrative and Comparative Biology*, 61, 1291–1309. https://doi.org/10.1093/icb/icab135
Bierne, N., Welch, J., Loire, E., Bonhomme, F., & David, P. (2011). The coupling hypothesis: Why genome scans may fail to map local adaptation genes. *Molecular Ecology*, 20(10), 2044–2072. https://doi.org/10.1111/j.1365-294X.2011.05080.x
Bolger, A. M., Lohse, M., & Usadel, B. (2014). Trimmomatic: A flexible trimmer for Illumina sequence data. *Bioinformatics*, 30(15), 2114–2120. https://doi.org/10.1093/bioinformatics/btu170
Bouckaert, R., Heled, J., Kühnert, D., Vaughan, T., Wu, C. -H., Xie, D., Suchard, M. A., Rambaut, A., & Drummond, A. J. (2014). BEAST 2: A software platform for Bayesian evolutionary analysis. *PLoS Computational Biology*, 10(4), e1003537. https://doi.org/10.1371/journal.pcbi.1003537
Brumfield, R. T., Jernigan, R. W., McDonald, D. B., & Braun, M. J. (2001). Evolutionary implications of divergent clines in an avian (*Manacus*: Aves) hybrid zone. *Evolution*, 55(10), 2070–2087. https://doi.org/10.1111/j.0014-3820.2001.tb01322.x
Bryant, D., & Moulton, V. (2004). Neighbor-net: An agglomerative method for the construction of phylogenetic networks. *Molecular Biology and Evolution*, 21(2), 255–265. https://doi.org/10.1093/molbev/msh018
Buggs, R. (2007). Empirical study of hybrid zone movement. *Heredity*, 99, 301–312. https://doi.org/10.1038/sj.hdy.6800997
Caballero, M., Lozano-García, S., Vázquez-Selem, L., & Ortega, B. (2010). Evidencias de cambio climático y ambiental en registros glaciales y en cuencas lacustres del centro de México durante el último máximo glacial. *Boletín de la Sociedad Geológica Mexicana*, 62, 359–377.
Carling, M. D., & Brumfield, R. T. (2008). Haldane's rule in an avian system: Using cline theory and divergence population genetics to test for differential introgression of mitochondrial, autosomal, and sex-linked loci across the *Passerina* bunting hybrid zone. *Evolution*, 62(10), 2600–2615. https://doi.org/10.1111/j.1558-5646.2008.00477.x
Carling, M. D., & Zuckerberg, B. (2011). Spatio-temporal changes in the genetic structure of the *Passerina* bunting hybrid zone. *Molecular Ecology*, 20(6), 1166–1175. https://doi.org/10.1111/j.1365-294X.2010.04987.x
Cui, R., Schumer, M., Kruesi, K., Walter, R., Andolfatto, P., & Rosenthal, G. G. (2013). Phylogenomics reveals extensive reticulate evolution in *Xiphophorus* fishes. *Evolution*, 67(8), 2166–2179. https://doi.org/10.1111/evo.12099
DeRaad, D. A., McCormack, J. E., Chen, N., Peterson, A. T., & Moyle, R. G. (2022). Combining species delimitation, species trees, and tests for gene flow clarifies complex speciation in scrub-jays. *Systematic Biology*, 71(6), 1453–1470. https://doi.org/10.1093/sysbio/syac034
DeRaad, D. A. (2022). snpfiltr: An R package for interactive and reproducible SNP filtering. *Molecular Ecology Resources*, 22, 2443–2453. https://doi.org/10.1111/1755-0998.13618
Derryberry, E. P., Derryberry, G. E., Maley, J. M., & Brumfield, R. T. (2014). HZAR: Hybrid zone analysis using an R software package. *Molecular Ecology Resources*, 14(3), 652–663. https://doi.org/10.1111/1755-0998.12209
Dobzhansky, T. (1955). *Evolution, genetics, and man*. John Wiley & Sons.
Dowling, T. E., & Secor, C. L. (1997). The role of hybridization and introgression in the diversification of animals. *Annual Review of Ecology and Systematics*, 28, 593–619. https://doi.org/10.1146/annurev.ecolsys.28.1.593
Endler, J. A. (1977). *Geographic variation, speciation and clines*. Princeton University Press. https://doi.org/10.1146/annurev.ecolsys.28.1.593
Excoffier, L., Marchi, N., Marques, D. A., Matthey-Doret, R., Gouy, A., & Sousa, V. C. (2021). fastsimcoal2: Demographic inference under complex evolutionary scenarios. *Bioinformatics*, 37(24), 4882–4885. https://doi.org/10.1093/bioinformatics/btab468
Faircloth, B. (2014). Illumiprocessor: A trimmomatic wrapper for parallel adapter and quality trimming. https://github.com/faircloth-lab/illumiprocessor.
Faircloth, B. C. (2016). PHYLUCE is a software package for the analysis of conserved genomic loci. *Bioinformatics*, 32(5), 786–788. https://doi.org/10.1093/bioinformatics/btv646
Faircloth, B. C., McCormack, J. E., Crawford, N. G., Harvey, M. G., Brumfield, R. T., & Glenn, T. C. (2012). Ultraconserved elements anchor thousands of genetic markers spanning multiple evolutionary timescales. *Systematic Biology*, 61(5), 717–726. https://doi.org/10.1093/sysbio/sys004
Ferreira, M. S., Jones, M. R., Callahan, C. M., Farelo, L., Tolesa, Z., Suchentrunk, F., Boursot, P., Mills, L. S., Alves, P. C., Good, J. M., & Melo-Ferreira, J. (2021). The legacy of recurrent introgression during the radiation of hares. *Systematic Biology*, 70(3), 593–607. https://doi.org/10.1093/sysbio/syaa088
Feliner, G. N., Álvarez, I., Fuertes-Aguilar, J., Heuertz, M., Marques, I., Moharrek, F., Piñeiro, R., Riina, R., Rosselló, J., & Soltis, P. (2017). Is homoploid hybrid speciation that rare? An empiricist's view. *Heredity*, 118, 513–516. https://doi.org/10.1038/hdy.2017.7
Glenn, T. C., Nilsen, R. A., Kieran, T. J., Sanders, J. G., Bayona-Vásquez, N. J.N. J., Finger, J. W., Pierson, T. W., Bentley, K. E., Hoffberg, S. L., Louha, S., Garcia-De Leon, F. J., Del Rio Portilla, M. A., Reed, K. D., Anderson, J. L., Meece, J. K., Aggrey, S. E., Rekaya, R., Alabady, M., Belanger, M., … Faircloth, B. C. (2019). Adapterama I: Universal stubs and primers for 384 unique dual-indexed or 147,456 combinatorially-indexed Illumina libraries (iTru & iNext). *PeerJ*, 7, e7755. https://doi.org/10.7717/peerj.7755
Gompert, Z., & Buerkle, C. (2010). INTROGRESS: A software package for mapping components of isolation in hybrids. *Molecular Ecology Resources*, 10, 378–384. https://doi.org/10.1111/j.1755-0998.2009.02733.x
Good, J. M., Demboski, J. R., Nagorsen, D. W., & Sullivan, J. (2003). Phylogeography and introgressive hybridization: Chipmunks (genus *Tamias*) in the northern Rocky Mountains. *Evolution*, 57(8), 1900–1916. https://doi.org/10.1111/j.0014-3820.2003.tb00597.x
Gowen, F. C., Maley, J. M., Cicero, C., Peterson, A. T., Faircloth, B. C., Warr, T. C., & McCormack, J. E. (2014). Speciation in Western Scrub-Jays, Haldane's rule, and genetic clines in secondary contact. *BMC Evolutionary Biology*, 14, 1–15. https://doi.org/10.1186/1471-2148-14-135
Grant, V. (1981). *Plant speciation*. Columbia University Press.
Griffiths, R. C., & Marjoram, P. (1996). Ancestral inference from samples of DNA sequences with recombination. *Journal of Computational Biology*, 3, 479–502. https://doi.org/10.1089/cmb.1996.3.479
Guiller, A., Coutellec-Vreto, M. -A., & Madec, L. (1996). Genetic relationships among suspected contact zone populations of *Helix aspersa* (Gastropoda: Pulmonata) in Algeria. *Heredity*, 77(2), 113–129. https://doi.org/10.1038/hdy.1996.116
Hahn, C., Bachmann, L., & Chevreux, B. (2013). Reconstructing mitochondrial genomes directly from genomic next-generation sequencing reads—A baiting and iterative mapping approach. *Nucleic Acids Research*, 41(13): e129–e129. https://doi.org/10.1093/nar/gkt371

Hamilton, J. A., Lexer, C., & Aitken, S. N. (2013). Genomic and phenotypic architecture of a spruce hybrid zone (*P. icea sitchensis* × *P. glauca*). *Molecular Ecology*, 22(3), 827–841. https://doi.org/10.1111/mec.12007

Harrison, R. G., & Harrison, R. G. (1993). *Hybrid zones and the evolutionary process*. Oxford University Press.

Hermansen, J. S., Sæther, S. A., Elgvin, T. O., Borge, T., Hjelle, E., & Sætre, G. P. (2011). Hybrid speciation in sparrows I: Phenotypic intermediacy, genetic admixture and barriers to gene flow. *Molecular Ecology*, 20, 3812–3822. https://doi.org/10.1111/j.1365-294X.2011.05183.x

Hewitt, G. M. (1988). Hybrid zones-natural laboratories for evolutionary studies. *Trends in Ecology & Evolution*, 3(7), 158–167. https://doi.org/10.1016/0169-5347(88)90033-X

Hill, G. E., & Johnson, J. D. (2013). The mitonuclear compatibility hypothesis of sexual selection. *Proceedings of the Royal Society B: Biological Sciences*, 280(1768), 20131314. https://doi.org/10.1098/rspb.2013.1314

Hofman, S., & Szymura, J. M. (2007). Limited mitochondrial DNA introgression in a *Bombina* hybrid zone. *Biological Journal of the Linnean Society*, 91(2), 295–306. https://doi.org/10.1111/j.1095-8312.2007.00795.x

Howell, S. N., & Webb, S. (1995). *A guide to the birds of Mexico and northern Central America*. Oxford University Press.

Huson, D. H., & Bryant, D. (2006). Application of phylogenetic networks in evolutionary studies. *Molecular Biology and Evolution*, 23(2), 254–267. https://doi.org/10.1093/molbev/msj030

Jaarola, M., Tegelström, H., & Fredga, K. (1997). A contact zone with noncoincident clines for sex-specific markers in the field vole (*Microtus agrestis*). *Evolution*, 51(1), 241–249. https://doi.org/10.1111/j.1558-5646.1997.tb02405.x

Jiggins, C. D., Salazar, C., Linares, M., & Mavarez, J. (2008). Hybrid trait speciation and *Heliconius* butterflies. *Philosophical Transactions of the Royal Society B: Biological Sciences*, 363(1506), 3047–3054. https://doi.org/10.1098/rstb.2008.0065

Jofre, G. I., & Rosenthal, G. G. (2021). A narrow window for geographic cline analysis using genomic data: Effects of age, drift, and migration on error rates. *Molecular Ecology Resources*, 21(7), 2278–2287. https://doi.org/10.1111/1755-0998.13428

Jombart, T. (2008). adegenet: A R package for the multivariate analysis of genetic markers. *Bioinformatics*, 24(11), 1403–1405. https://doi.org/10.1093/bioinformatics/btn129

Kearns, A. M., Restani, M., Szabo, I., Schrøder-Nielsen, A., Kim, J. A., Richardson, H. M., Marzluff, J. M., Fleischer, R. C., Johnsen, A., & Omland, K. E. (2018). Genomic evidence of speciation reversal in ravens. *Nature Communications*, 9, 1–13. https://doi.org/10.1038/s41467-018-03294-w

Kearse, M., Moir, R., Wilson, A., Stones-Havas, S., Cheung, M., Sturrock, S., Buxton, S., Cooper, A., Markowitz, S., Duran, C., Thierer, T., Ashton, B., Meintjes, P., & Drummond, A. (2012). Geneious Basic: An integrated and extendable desktop software platform for the organization and analysis of sequence data. *Bioinformatics*, 28(12), 1647–1649. https://doi.org/10.1093/bioinformatics/bts199

Kingston, S. E., Jernigan, R. W., Fagan, W. F., Braun, D., & Braun, M. J. (2012). Genomic variation in cline shape across a hybrid zone. *Ecology and Evolution*, 2(11), 2737–2748. https://doi.org/10.1002/ece3.375

Kingston, S. E., Navarro-Sigüenza, A. G., García-Trejo, E. A., Vázquez-Miranda, H., Fagan, W. F., & Braun, M. J. (2014). Genetic differentiation and habitat connectivity across towhee hybrid zones in Mexico. *Evolutionary Ecology*, 28, 277–297. https://doi.org/10.1007/s10682-013-9673-8

Kingston, S. E., Parchman, T., Gompert, Z., Buerkle, C., & Braun, M. J. (2017). Heterogeneity and concordance in locus-specific differentiation and introgression between species of towhees. *Journal of Evolutionary Biology*, 30, 474–485. https://doi.org/10.1111/jeb.13033

Korunes, K. L., & Samuk, K. (2021). pixy: Unbiased estimation of nucleotide diversity and divergence in the presence of missing data. *Molecular Ecology Resources*, 21(4), 1359–1368. https://doi.org/10.1111/1755-0998.13326

Kozak, K. M., Joron, M., McMillan, W. O., & Jiggins, C. D. (2021). Rampant genome-wide admixture across the *Heliconius* radiation. *Genome Biology and Evolution*, 13(7), evab099. https://doi.org/10.1093/gbe/evab099

Knaus, B. J., & Grünwald, N. J. (2017). vcfr: A package to manipulate and visualize variant call format data in R. *Molecular Ecology Resources*, 17(1), 44–53. https://doi.org/10.1111/1755-0998.12549

Lamichhaney, S., Han, F., Webster, M. T., Andersson, L., Grant, B. R., & Grant, P. R. (2018). Rapid hybrid speciation in Darwin's finches. *Science*, 359(6372), 224–228. https://doi.org/10.1126/science.aao4593

Leaché, A. D., Grummer, J. A., Harris, R. B., & Breckheimer, I. K. (2017). Evidence for concerted movement of nuclear and mitochondrial clines in a lizard hybrid zone. *Molecular Ecology*, 26(8), 2306–2316. https://doi.org/10.1111/mec.14033

Leavenworth, W. C. (1946). A preliminary study of the vegetation of the region between Cerro Tancítaro and the Río Tepalcatepec, Michoacán, Mexico. *American Midland Naturalist*, 36(1), 137–206. https://doi.org/10.2307/2421625

Leigh, J. W., & Bryant, D. (2015). POPART: Full-feature software for haplotype network construction. *Methods in Ecology and Evolution*, 6(9), 1110–1116. https://doi.org/10.1111/2041-210x.12410

Li, H., & Durbin, R. (2009). Fast and accurate short read alignment with Burrows–Wheeler transform. *Bioinformatics*, 25(14), 1754–1760. https://doi.org/10.1093/bioinformatics/btp324

Li, H., Handsaker, B., Wysoker, A., Fennell, T., Ruan, J., Homer, N., Marth, G., Abecasis, G., & Durbin, R.; 1000 Genome Project Data Processing Subgroup (2009). The sequence alignment/map format and SAMtools. *Bioinformatics*, 25(16), 2078–2079. https://doi.org/10.1093/bioinformatics/btp352

Linck, E., & Battey, C. (2019). Minor allele frequency thresholds strongly affect population structure inference with genomic data sets. *Molecular Ecology Resources*, 19, 639–647. https://doi.org/10.1111/1755-0998.12995

Lipshutz, S. E., Meier, J. I., Derryberry, G. E., Miller, M. J., Seehausen, O., & Derryberry, E. P. (2019). Differential introgression of a female competitive trait in a hybrid zone between sex-role reversed species. *Evolution*, 73(2), 188–201. https://doi.org/10.1111/evo.13675

Mallet, J. (2007). Hybrid speciation. *Nature*, 446(7133), 279–283. https://doi.org/10.1038/nature05706

Mallet, J., & Barton, N. H. (1989). Strong natural selection in a warning-color hybrid zone. *Evolution*, 43(2), 421–431. https://doi.org/10.1111/j.1558-5646.1989.tb04237.x

Mayr, E. (1963). *Animal species and evolution*. Belknap Press, Harvard University.

McCormack, J. E., Tsai, W. L., & Faircloth, B. C. (2016). Sequence capture of ultraconserved elements from bird museum specimens. *Molecular Ecology Resources*, 16(5), 1189–1203. https://doi.org/10.1111/1755-0998.12466

McDonald, D. B., Clay, R. P., Brumfield, R. T., & Braun, M. J. (2001). Sexual selection on plumage and behavior in an avian hybrid zone: Experimental tests of male-male interactions. *Evolution*, 55(7), 1443–1451. https://doi.org/10.1111/j.0014-3820.2001.tb00664.x

McKenna, A., Hanna, M., Banks, E., Sivachenko, A., Cibulskis, K., Kernytsky, A., Garimella, K., Altshuler, D., Gabriel, S., Daly, M., & DePristo, M. A. (2010). The genome analysis toolkit: A mapreduce framework for analyzing next-generation DNA sequencing data. *Genome Research*, 20(9), 1297–1303. https://doi.org/10.1101/gr.107524.110

Meier, J. I., Marques, D. A., Mwaiko, S., Wagner, C. E., Excoffier, L., & Seehausen, O. (2017). Ancient hybridization fuels rapid cichlid fish adaptive radiations. *Nature Communications*, 8, 1–11. https://doi.org/10.1038/ncomms14363

Metcalfe, S. E., O'Hara, S. L., Caballero, M., & Davies, S. J. (2000). Records of Late Pleistocene–Holocene climatic change in Mexico—A

review. *Quaternary Science Reviews*, 19(7), 699–721. https://doi.org/10.1016/s0277-3791(99)00022-0
Nei, M. (1972). Genetic distance between populations. *American Naturalist*, 106(949), 283–292. https://doi.org/10.1086/282771
Feliner, G. N., Casacuberta, J., & Wendel, J. F. (2020). Genomics of evolutionary novelty in hybrids and polyploids. *Frontiers in Genetics*, 11, 792. https://doi.org/10.3389/fgene.2020.00792
O'Leary, S. J., Puritz, J. B., Willis, S. C., Hollenbeck, C. M., & Portnoy, D. S. (2018). These aren't the loci you'e looking for: Principles of effective SNP filtering for molecular ecologists. *Molecular Ecology*, 27, 3193–3206. https://doi.org/10.1111/mec.14792
Olave, M., Nater, A., Kautt, A., & Meyer, A. (2022). Early stages of sympatric homoploid hybrid speciation in crater lake cichlid fishes. *Nature Communications*, 13, 5893. https://doi.org/10.1038/s41467-022-33319-4
Ottenburghs, J. (2018). Exploring the hybrid speciation continuum in birds. *Ecology and Evolution*, 8(24), 13027–13034. https://doi.org/10.1002/ece3.4558
Pardo-Diaz, C., Salazar, C., Baxter, S. W., Merot, C., Figueiredo-Ready, W., Joron, M., McMillan, W. O., & Jiggins, C. D. (2012). Adaptive introgression across species boundaries in Heliconius butterflies. *PLoS Genetics*, 8(6), e1002752. https://doi.org/10.1371/journal.pgen.1002752
Parsons, T. J., Olson, S. L., & Braun, M. J. (1993). Unidirectional spread of secondary sexual plumage traits across an avian hybrid zone. *Science*, 260(5114), 1643–1646. https://doi.org/10.1126/science.260.5114.1643
Pembleton, L. W., Cogan, N. O., & Forster, J. W. (2013). StAMPP: An R package for calculation of genetic differentiation and structure of mixed-ploidy level populations. *Molecular Ecology Resources*, 13(5), 946–952. https://doi.org/10.1111/1755-0998.12129
Petkova, D., Novembre, J., & Stephens, M. (2016). Visualizing spatial population structure with estimated effective migration surfaces. *Nature Genetics*, 48(1), 94–100. https://doi.org/10.1038/ng.3464
Poelstra, J. W., Vijay, N., Bossu, C. M., Lantz, H., Ryll, B., Müller, I., Baglione, V., Unneberg, P., Wikelski, M., Grabherr, M. G., & Wolf, J. B. W. (2014). The genomic landscape underlying phenotypic integrity in the face of gene flow in crows. *Science*, 344(6190), 1410–1414. https://doi.org/10.1126/science.1253226
Polechová, J., & Barton, N. (2011). Genetic drift widens the expected cline but narrows the expected cline width. *Genetics*, 189(1), 227–235. https://doi.org/10.1534/genetics.111.129817
Pudlo, P., Marin, J. -M., Estoup, A., Cornuet, J. -M., Gautier, M., & Robert, C. P. (2016). Reliable ABC model choice via random forests. *Bioinformatics*, 32(6), 859–866. https://doi.org/10.1093/bioinformatics/btv684
Racimo, F., Sankararaman, S., Nielsen, R., & Huerta-Sánchez, E. (2015). Evidence for archaic adaptive introgression in humans. *Nature Reviews Genetics*, 16(6), 359–371. https://doi.org/10.1038/nrg3936
Rambaut, A., Drummond, A. J., Xie, D., Baele, G., & Suchard, M. A. (2018). Posterior summarization in Bayesian phylogenetics using Tracer 1.7. *Systematic Biology*, 67(5), 901–904. https://doi.org/10.1093/sysbio/syy032
R Core Team. 2019. *R: A language and environment for statistical computing*. R Foundation for Statistical Computing, Vienna, Austria.
Rising, J. D. 2020. Collared Towhee (*Pipilo ocai*). In A. E. J. del Hoyo, J. Sargatal, D. A. Christie, & E. de Juana (Eds.). *Handbook of the birds of the world alive*. Lynx Edicions.
Royer, A. M., Waite-Himmelwright, J., & Smith, C. I. (2020). Strong selection against early generation hybrids in Joshua Tree hybrid zone not explained by pollinators alone. *Frontiers in Plant Science*, 11, 640. https://doi.org/10.3389/fpls.2020.00640
Ryan, S. F., Deines, J. M., Scriber, J. M., Pfrender, M. E., Jones, S. E., Emrich, S. J., & Hellmann, J. J. (2018). Climate-mediated hybrid zone movement revealed with genomics, museum collection, and simulation modeling. *Proceedings of the National Academy of Sciences*, 115, E2284–E2291. https://doi.org/10.1073/pnas.1714950115
Schilthuizen, M., & Gittenberger, E. (1994). Parallel evolution of an sAat-'hybrizyme' in hybrid zones in *Albinaria hippolyti* (Boettger). *Heredity*, 73(3), 244–248. https://doi.org/10.1038/hdy.1994.129
Schumer, M., Rosenthal, G. G., & Andolfatto, P. (2014). How common is homoploid hybrid speciation? *Evolution*, 68(6), 1553–1560. https://doi.org/10.1111/evo.12399
Schumer, M., Xu, C., Powell, D. L., Durvasula, A., Skov, L., Holland, C., Blazier, J. C., Sankararaman, S., Andolfatto, P., Rosenthal, G. G., & Przeworski, M. (2018). Natural selection interacts with recombination to shape the evolution of hybrid genomes. *Science*, 360(6389), 656–660. https://doi.org/10.1126/science.aar3684
Seehausen, O. (2004). Hybridization and adaptive radiation. *Trends in Ecology & Evolution*, 19(4), 198–207. https://doi.org/10.1016/j.tree.2004.01.003
Selz, O. M., & Seehausen, O. (2019). Interspecific hybridization can generate functional novelty in cichlid fish. *Proceedings of the Royal Society of London. Series B, Biological Sciences*, 286, 20191621. https://doi.org/10.1098/rspb.2019.1621
Sequeira, F., Arntzen, J. W., Gulik, D. van, Hajema, S., Diaz, R. L., Wagt, M., & Riemsdijk, I. van (2022). Genetic traces of hybrid zone movement across a fragmented habitat. *Journal of Evolutionary Biology*, 35, 400–412. https://doi.org/10.1111/jeb.13982
Sibley, C. G. (1950). *Species formation in the red-eyed towhees of Mexico*. University of California Press.
Sibley, C. G. (1954). Hybridization in the red-eyed towhees of Mexico. *Evolution*, 8(3), 252–290. https://doi.org/10.2307/2405443
Slatkin, M. (1973). Gene flow and selection in a cline. *Genetics*, 75(4), 733–756. https://doi.org/10.1093/genetics/75.4.733
Smith, M. L., & Carstens, B. C. (2020). Process-based species delimitation leads to identification of more biologically relevant species. *Evolution*, 74(2), 216–229. https://doi.org/10.1111/evo.13878
Soltis, P. (2013). Hybridization, speciation and novelty. *Journal of Evolutionary Biology*, 26, 291–293. https://doi.org/10.1111/jeb.12095
Stein, A. C., & Uy, J. A. C. (2006). Unidirectional introgression of a sexually selected trait across an avian hybrid zone: a role for female choice? *Evolution*, 60(7), 1476–1485. https://doi.org/10.1554/05-575.1
Swenson, N. G., & Howard, D. J. (2005). Clustering of contact zones, hybrid zones, and phylogeographic breaks in North America. *American Naturalist*, 166, 581–591. https://doi.org/10.1086/491688
Taylor, S. A., Curry, R. L., White, T. A., Ferretti, V., & Lovette, I. (2014). Spatiotemporally consistent genomic signatures of reproductive isolation in a moving hybrid zone. *Evolution*, 68(11), 3066–3081. https://doi.org/10.1111/evo.12510
Taylor, S. A., & Larson, E. L. (2019). Insights from genomes into the evolutionary importance and prevalence of hybridization in nature. *Nature Ecology & Evolution*, 3(2), 170–177. https://doi.org/10.1038/s41559-018-0777-y
Toews, D. P., Taylor, S. A., Vallender, R., Brelsford, A., Butcher, B. G., Messer, P. W., & Lovette, I. J. (2016). Plumage genes and little else distinguish the genomes of hybridizing warblers. *Current Biology*, 26, 2313–2318. https://doi.org/10.1016/j.cub.2016.06.034
Tsai, W. L., Schedl, M. E., Maley, J. M., & McCormack, J. E. (2020). More than skin and bones: comparing extraction methods and alternative sources of DNA from avian museum specimens. *Molecular Ecology Resources*, 20, 1220–1227. https://doi.org/10.1111/1755-0998.13077
Wang, Z., Jiang, Y., Bi, H., Lu, Z., Ma, Y., Yang, X., Chen, N., Tian, B., Liu, B., Mao, X., Ma, T., DiFazio, S. P., Hu, Q., Abbott, R. J., & Liu, J. (2021b). Hybrid speciation via inheritance of alternate alleles of parental isolating genes. *Molecular Plant*, 14(2), 208–222. https://doi.org/10.1016/j.molp.2020.11.008
Wang, S., Ore, M. J., Mikkelsen, E. K., Lee-Yaw, J., Toews, D. P., Rohwer, S., & Irwin, D. (2021a). Signatures of mitonuclear coevolution in a warbler species complex. *Nature Communications*, 12, 1–11. https://doi.org/10.1038/s41467-021-24586-8
Wang, S., Rohwer, S., Delmore, K., & Irwin, D. E. (2019). Cross-decades stability of an avian hybrid zone. *Journal of Evolutionary Biology*, 32(11), 1242–1251. https://doi.org/10.1111/jeb.13524
Wang, S., Rohwer, S., Zwaan, D. R., Toews, D. P., Lovette, I. J., Mackenzie, J., & Irwin, D. (2020). Selection on a small genomic region

underpins differentiation in multiple color traits between two warbler species. *Evolution Letters*, 4, 502–515. https://doi.org/10.1002/evl3.198

Watts, W. A., & Bradbury, J. P. (1982). Paleoecological studies at Lake Patzcuaro on the west-central Mexican Plateau and at Chalco in the Basin of Mexico. *Quaternary Research*, 17(1), 56–70. https://doi.org/10.1016/0033-5894(82)90045-x

While, G. M., Michaelides, S., Heathcote, R. J., MacGregor, H. E., Zajac, N., Beninde, J., Carazo, P., Perez i de Lanuza, G., Sacchi, R., & Zuffi, M. A. (2015). Sexual selection drives asymmetric introgression in wall lizards. *Ecology Letters*, 18, 1366–1375. https://doi.org/10.1111/ele.12531

Wickham, H. (2016). *ggplot2: Elegant graphics for data analysis*. Springer-Verlag.

Wielstra, B. (2019). Historical hybrid zone movement: More pervasive than appreciated. *Journal of Biogeography*, 46(7), 1300–1305. https://doi.org/10.1111/jbi.13600